HHS Public Access

Author manuscript

J Cell Physiol. Author manuscript; available in PMC 2015 August 07.

Published in final edited form as:

J Cell Physiol. 2015 February ; 230(2): 378–394. doi:10.1002/jcp.24722.

Hydrogen sulfide epigenetically attenuates homocysteine-induced mitochondrial toxicity mediated through NMDA receptor in mouse brain endothelial (bEnd3) cells†

Pradip K. Kamat, **Anuradha Kalani**, **Suresh C. Tyagi**, and **Neetu Tyagi**

Department of Physiology and Biophysics, School of Medicine, University of Louisville, and Louisville, KY 40202, USA

Abstract

Previously we have showed that homocysteine (Hcy) caused oxidative stress and altered mitochondrial function. Hydrogen sulphide (H_2S) has potent anti-inflammatory, anti-oxidative and anti-apoptotic effects. Therefore, in the present study we examined whether H_2S ameliorates Hcy-induced mitochondrial toxicity which led to endothelial dysfunction in part, by epigenetic alterations in mouse brain endothelial cells (bEnd3). The bEnd3 cells were exposed to 100μM Hcy treatment in the presence or absence of 30μM NaHS (donor of H_2S) for 24hrs. Hcy-activate NMDA receptor and induced mitochondrial toxicity by increased levels of Ca^{2+}, NADPH-oxidase-4 (NOX-4) expression, mitochondrial dehydrogenase activity and decreased the level of nitrate, superoxide dismutase (SOD-2) expression, mitochondria membrane potentials, ATP production. To confirm the role of epigenetic, 5′-azacitidine (an epigenetic modulator) treatment was given to the cells. Pretreatment with NaHS (30μM) attenuated the Hcy-induced increased expression of DNMT1, DNMT3a, Ca^{2+} and decreased expression of DNMT3b in bEND3 cells. Furthermore, NaHS treatment also enhanced mitochondrial oxidative stress (NOX4, ROS, and NO) and restored ATP that indicates its protective effects against mitochondrial toxicity. Additional, NaHS significantly alleviated Hcy-induced LC3-I/II, CSE, Atg3/7 and low p62 expression which confirm its effect on mitophagy. Likewise, NaHS also restored level of eNOS, CD31, VE-Cadherin and ET-1 and maintains endothelial function in Hcy treated cells. Molecular inhibition of NMDA receptor by using small interfering RNA showed protective effect whereas inhibition of H_2S production by propargylglycine (PG) (inhibitor of enzyme CSE) showed mitotoxic effect. Taken together, results demonstrate that, administration of H_2S protected the cells from HHcy-induced mitochondrial toxicity and endothelial dysfunction.

Keywords

Mitochondrial Toxicity; DNA methylation; Free radicals; autophagy; H_2S; Endothelial cell toxicity

†This article has been accepted for publication and undergone full peer review but has not been through the copyediting, typesetting, pagination and proofreading process, which may lead to differences between this version and the Version of Record. Please cite this article as doi: [10.1002/jcp.24722]

Address for Correspondence: Neetu Tyagi, Ph.D., Department of Physiology and Biophysics, Health Sciences Center, A-1201, University of Louisville, Louisville, KY 40202; Phone: 502-852-4145, Fax: 502-852-6239, n0tyag01@louisville.edu.

Introduction

Homocysteine (Hcy) is a non-protein amino acid derived from the metabolic demethylation of dietary methionine. An elevation of plasma Hcy above 15 μmol/l, is defined as hyperhomocysteinemia (HHcy) and is an independent risk factor for cerebrovascular diseases such as dementia, Alzheimer's disease (AD), and stroke (Faraci and Lentz, 2004; Levonen et al., 2000; Obeid and Herrmann, 2006). Hcy can also stimulate a cascade of vascular dysfunction including alterations of endothelial functions and an increased accumulation of extracellular matrix (Chang et al., 2008; Austin et al., 2004). These unfavorable vascular dysfunctions may be mediated by increased production of reactive oxygen species (ROS) and nitrogen species which have been strongly implicated in the development of micro and macro vascular diseases (Eberhardt et al., 2000; Tyagi et al., 2005). ROS generation from mitochondria has been associated with various forms of signaling because mitochondria are responsible for the ROS formation in most of the cells. A necessary gap is there to explore the mechanism by which the Hcy affects vascular function. Whether there is a receptor to mediate intracellular signal transduction. Neurons as well as endothelial cells contain a receptor for Hcy i.e N-methyl D- aspartate (NMDA). Recent studies have demonstrated that NMDA receptors (NMDA-R) have a high affinity for Hcy binding and Hcy has been found to bind to the glutamate site of the NMDA-R1 (Doronzo et al., 2009). The activation of the NMDA receptor initiates several events, including calcium influx, activation of nitric oxide synthase, and formation of superoxide anion ($O_2^{\cdot -}$) leading to cell death (Duchene et al., 2004; Rai et al., 2013; Lipton et al., 2004; Poddar and Paul, 2009). This receptor also exists in the brain arterial vascular bed and serves as the initial entry point for transporting Hcy into endothelial cells (Chen et al., 2010), and their over stimulation is associated with endothelial dysfunction. However there is a controversy about its association between HHcy and vascular disease. The possible mechanism includes induction of free radicals formation and activation of NMDA-R1 by HHcy.

The maintenance of DNA methylation patterns in different genomic regions is catalyzed by the DNA methyltransferase (DNMT) including DNMT1, 3a and 3b. DNMTs are the enzymes which is responsible for cytosine methylation (Reinhart and Chaillet, 2005; Cirio et al., 2008). Abnormal epigenetic modifications mediated by mechanisms such as DNA methylation, core histone methylation, and acetylation are known to play important roles in development of vascular disease (Santos-Reboucas and Pimentel, 2007; Wilson et al., 2007). However, whether these mechanisms are involved in mitochondrial toxicity remains unknown.

Hydrogen sulfide (H_2S) was found to be produced endogenously from the sulfur containing amino acid L-cysteine by the help of the enzymes cystathionine β-synthase (CBS), cystathionine γ-lyase (CSE), and 3-mercaptopyruvate sulfurtransferase (3MST) (Kimura, 2011). However, emerging evidence indicates the important physiological effects of H_2S as a novel type of endogenous neural regulatory factor and gaseous mediator (Lowicka and Beltowski, 2007). In particular, it has been demonstrated that the administration of H_2S significantly ameliorates neurovascular dysfunction (Kamat et al., 2013) and can also protect the brain's endothelial cells from oxidative stress (White et al., 2001). These multiple

protective properties suggest that H_2S works as a safeguard and acts as a neuromodulator in the brain. Tyagi et al. (2009) suggested that H_2S acts as an endogenous scavenger for ROS. However, the role of H_2S on mitochondrial toxicity in endothelial cells through epigenetic modification is still unclear.

Endothelial cells play a crucial role in blood brain barrier function and any alteration in its function could have deleterious effects in neurovascular diseases (Weiss et al., 2009). Previous report form our laboratory demonstrated that HHcy resulted in significant increase in brain permeability and altered mitochondrial function (Kalani et al., 2013). Therefore, attention has been focused on the mitochondrial toxicity leading to vascular complications by controlling the intra-mitochondrial redox state. Mitochondria are of particular interest because they are known to be involved in the neurodegenerative process including micro-vascular complications (Kamat et al., 2011; Tyagi et al., 2009). Considering the important role of mitochondria in neurodegenerative diseases and elucidating the mechanisms by which HHcy causes functional alterations in endothelial cells is necessary.

Therefore, the purpose of this study was to determine a potential role of H_2S in Hcy-mediated ROS production which promotes endothelial cell dysfunction in part by disturbing membrane potential, which results in subsequent Ca^{2+} influx alteration leading to mitochondrial cell toxicity via epigenetic modification. The treatment with NaHS/H_2S can prevent these alterations.

Material and Methods

Reagents and Antibodies

DL-Homocysteine (Hcy), DL –Propargylglycine (PG) and NaHS were purchased from Sigma Aldrich (St. Louis, MO). Hydrogen peroxide (H_2O_2), and Tween-20 were obtained from Fischer Scientific (Fair Lawn, New Jersey). Dulbecco's modified Eagle's medium (DMEM), fetal bovine serum (FBS), penicillin, and streptomycin were procured from American Type Culture Collection (ATCC). Polyclonal antibody to DNMT1, DNMT3a, DNMT3b, NMDA-R1, NOX4, SOD2, LC3, LC3-I/II, CSE, Atg3/7 p62, eNOS, VE-cadherin, CD31 and Endothelin 1 were procured from ABCAM (Cambridge, MA, USA) and Santa Cruz Biotechnology (Santa Cruz, CA). 4′, 6-diamidino-2-phenylindole (DAPI), ATP assay Kit, JC-1 and 2′, 7′-dichlorodihydrofluoresceindiacetate (H_2DCF-DA), MitoSOX Red and MitoTracker green FM were purchased from Invitrogen (Eugene, OR). The NMDA-R siRNA (cat no. SI00172977) and control siRNA (cat no. 1027310) was procured from Qiagen (Qiagen, Valencia, CA, USA).

Methods

Cell Culture

In the present study we used mouse brain endothelial cells (bEND3; American Type Culture Collection, Manassas, VA), were grown in 75cm^2 flasks in DMEM medium which contained 0.45% glucose, 0.37% $NaHCO_3$, 4mM glutamine, 10% FBS, 100 μg/ml penicillin, and 100 μg/ml streptomycin. The bEND3 were grown to confluence before being trypsinized into a complete media. The cells were then pelleted at 100g for 5 minutes. Once

the pellet was formed, the bEND3 were re-suspended in complete media and seeded for experiment. The cells were grown in a humidified incubator at 37°C with 5% CO_2. Cell treatments were performed in incomplete media. After 24 hr of treatment with Hcy, NaHS, 5-Aza and H_2O_2 cells were harvested and used for molecular and biochemical staining.

Treatments: The experimental groups were as following

Control (CT), 5μM Hcy, 100μM Hcy, 100μM Hcy + 30μM NaHS, 30μM NaHS alone, 100μM H_2O_2 alone and 100μM Hcy + 10μM 5-Aza cytidine, 100μM Hcy + 0.25μM PG, 100μM Hcy + 10nM siRNA, 10nM control siRNA, NaHS+PG, PG. The H_2O_2 was used as a positive control group for free radical generation. Stock solution of Hcy, NaHS and H_2O_2 was directly dissolved in incomplete DMEM medium. The cells were grown to 80% confluence and then treated with different chemical compounds. Treatment was provided in incomplete media for 24 hours in the same condition as they were raised. Since, 5μM Hcy did not affect any changes in cellular functions therefore; most of the experiments were performed at 100μM Hcy treatment.

Mitochondrial dehydrogenase enzyme activity assay

MTT(3-(4,5-dimethylthiazol-2-yl)-2,5-diphenyltetrazolium bromide, a yellow tetrazole), is reduced to purple formazan in living cells) assay was used for mitochondrial dehydrogenase enzyme activity and experiments were carried out according to the method described by Kamat et al. (2011). Brie y cells were subjected to respective treatments for 24 h and then incubated with MTT dye in dark for 2 h at 37°C. After incubation, the media was discarded, and the pink-colored formazan crystals were dissolved in DMSO. The intensity of formazan was measured by spectrophotometer at 550 nm with reference wavelength of 630 nm.

In situ labeling of ROS through oxidized DCF

Oxidized DCF (reflecting the levels of H_2O_2 and $ONOO^-$) in cells was assessed by using the DCFH-DA assay as described previously (Tyagi et al., 2006). Briefly, cells were washed with PBS. Then cells were loaded with the probe DCFH-DA (5 μM) and incubated for 30 min at 37 °C in PBS, protected from light. After incubation the cells were again washed twice with fresh PBS to remove the excess DCF probe. Oxidized DCF images in cells were acquired by laser confocal microscope (FluoView 1000) at an excitation of 488 nm and emission of 525 nm in cells was quantified by confocal microscopy and expressed in arbitrary units.

In situ labeling of Mitochondrial ROS

To detect basal mitochondrial superoxide generation in in each treatment group, bEND3 cells were seeded in a 8-well chamber, grown to the appropriate confluence and cell treated for 24 hours. MitoSOX Red (Invitrogen, Eugene, OR), a cationic dye that fluoresces red when oxidized by mitochondrial superoxide was utilized. Briefly, cells (50,000 cells/well) were plated in glass chamber slides (Nunc, Rochester, NY) grown to the appropriate confluence and cell treated for 24 hours. After 24 h post-treatment, cells were treated in the dark with MitoSOX red (5uM) at 37°C for 20 min. Again cells were washed with cellular medium and incubate with cell per-meant Mito Tracker green probe (200nM) and kept at

37°C for 20 min and then cell washed and again incubated with DAPI (nuclear stain) for 20 min. later cells were fixed with 3.7% paraformaldehyde (PFA). Subsequently, cells were washed with cellular medium and imaged using the Olympus confocal laser scanning microscope (100x) with excitation/emission (510/580 nm) filters. All images were captured with equal exposure times and quantified using image pro- software (Image Lab).

Monodansylcadaverine (MDC) Staining

We performed MDC staining to examine the level of autophagy in different treatment groups. bEnd 3 were seeded in an 8-well chamber and treated with different compound used in our study model. After 24 hours of treatment, the media was aspirated and cells were stained with MDC at a concentration of 50 μM in PBS for 30 minutes. Afterwards, the cells were washed with PBS and examined using a confocal microscope (Olympus FV1000) at 525 nm wavelength emission. Using Fluoview software provided by the manufacturer, we gave virtual color to the images to view the autophagic vacuoles as blue. These vacuoles were labeled with MDC because it is a basic molecule with lipid affinity and therefore localizes to the acidic auto lysosomes by way of an ion-trapping mechanism (Vazquez and Colombo, 2009). The number of vacuoles formed was analyzed by Image Pro Plus software (Media Cybernetics, Bethesda, MD) by measuring the fluorescent intensity/density.

Membrane potential ($\Delta\psi p$)

Measurement of mitochondrial membrane potential was performed using the JC-1 (5,5′,6,6′-tetrachloro-1,1′,3,3′-tetraethylbenzimidazolylcarbocyanine iodide) dye (Molecular Probes, Invitrogen) as described previously (Tyagi et al., 2006). The cationic dye JC-1 accumulates and aggregates in intact mitochondria, emitting a bright red fluorescence, whereas, upon disruption of the mitochondrial membrane potential, the monomeric dye emits green fluorescence in the cytoplasm. Briefly, bEND3 cells were pre-treated with different treatment for 24 h and later used for membrane potential estimation. At 24 h post-treatment, cells were incubated with JC-1 dye (200 nM for 30 min) at 37°C in the dark. Subsequently, cells were washed with PBS two times for 5 minute each. After treatment images were taken using the Olympus laser scanning confocal microscope (100x) with excitation and emission wavelengths set at 485 and 595 nm respectively for red fluorescence, and 485 and 535 nm respectively for green fluorescence and the ratio of red signal to green signal was calculated.

ATP Estimation

ATP levels were determined by ATP assay kit [ATP Determination Kit (A22066), Molecular probe] according to manufacturer instruction. Briefly, cells was lysed in 100 μl of RIPA buffer and centrifuged at 12,000 × *g* for 10 min to pellet insoluble materials. The components of the reaction mixture were: [To make 10 mL of a standard reaction solution (8.9 mL dH2O); (Component E: 0.5 mL 20X Reaction Buffer); 0.1 mL 0.1 M DTT; 0.5 mL of 10 mM D-luciferin; 2.5 μL of firefly luciferase from 5 mg/mL stock solution]. The ATP level was expressed as (Pico mole/mg of protein).

Calcium ion estimation

Intracellular calcium level was measured by uorescence probe FURA-2 AM following the method of Grynkiewicz et al. bEND3 cells were seeded in a 6-well plates. After treatment for 24 h, medium was aspirated and cells were suspended in PBS for 1 h at 37 ° C in an incubator containing 5 μM FURA- 2AM as a nal concentration. PBS was removed and replaced with the fresh PBS. Fluorescence was read using a spectro uorometer at dual wave length Ex 340/380 nm and Em 510nm. Calcium level was calculated according to formula suggested by Grynkiewicz et al. (1985). Calcium level was expressed as percentage basal level of control.

Nitrite estimation

Total nitrite was estimated in the bEND3 cells using the Greiss reagent and served as an indicator of nitric oxide (NO) production (Green et al., 1982). 100 μl of Greiss reagent [1:1 solution of 1% sulphanilamide in 5% ortho-phosphoric acid, 0.1% napthaylamine diamine dihydrochloric acid and nitrate reductase (1U/ml) in water] was added to 100 μl of supernatant and absorbance was measured at 542 nm. Nitrite concentration was calculated using a standard curve for sodium nitrite and expressed in μg/mg protein.

Reverse Transcription-Polymerase Chain Reaction

bEND3 cells were seeded in 6-well plates and treatment was given for 24 h. After 24 h, RNA was isolated using Trizol Reagent (Gibco BRL) according to the manufacturer instructions. The quantity and quality of RNA was measured by using the instrument Nano Drop 1000 spectrophotometer. RT-PCR reaction was performed by using ImProm-II™ Reverse Transcription PCR system kit (Promega Corporation, Madison, WI). Complimentary DNA (cDNA) was prepared using 2 μg of the RNA. A reverse transcription program on the DNA Engine S1000 Thermal Cycler (Bio-Rad Laboratories, Hercules, CA) was used to make the cDNA. The program consisted of a denaturing cycle at 70°C for 6 minutes and then a reverse transcription cycle at 25°C for 2 minutes, 42°C for 50 minutes, 75°C for 5 minutes. Then 2 μl of cDNA (incubated with gene primers and nuclease free water for a final volume of 20 μl) from each sample was used for a gene amplification cycle at 95°C for 7 minutes (95°C for 50 seconds, 55°C for 1 minutes, 72°C for 1 minute) (35 cycle), 72°C for 5 minutes. Quantification of the amplicon was measured using Image Lab software (Bio-Rad Laboratories, Hercules, CA) and each sample was normalized with GAPDH.

qRT-PCR analysis for mitochondrial DNA damage

The transcript level of mitochondrial damage was determined in the cDNA sample by using quantitative real-time PCR. The PCR mixture (25 μl) contained 12.5 μl SYBR GREEN PCR master mix, 1 μl cDNA and 40 pmol and amplified through stratagene Mx3000p (Agilent Technologies, Santa Clara, CA, USA). The mitochondrial damage was normalized with GAPDH expression.

Western blotting

Variations in protein content of, DNMT1, DNMT3a, DNMT3b, p62, NMDA-R1, NOX4, CSE, LC3, LC3-I/II, Atg-3, Atg-7, eNOS, SOD2, VE-cadherin, CD31 and Endothelin 1 were assessed by Western blot method. Briefly, cells were washed twice with ice-cold PBS and lysed with ice-cold RIPA buffer (containing 5 mM of ethylenediamine-tetraacetic acid), which was supplemented with phenylmethylsulfonyl fluoride (1 mM) and protease inhibitor cocktail (1 μl/ml of lysis buffer). Protein content of the cell lysate was determined by using the Bradford assay. Equal amounts of protein (50 μg) were resolved on SDS-PAGE (8%, 10%, 15%) and transferred onto a polyvinylidene difluoride membrane. The blots were analyzed with Gel-Pro Analyzer software (Media Cybernetics, Silver Spring, MD) according to manufacturer instruction. To determine the protein expression for each treatment, the intensity of protein band was assessed by the integrated optical density (IOD). To account for possible differences in the protein load, the density of each band were (protein of interest) divided by the density of the respective of GAPDH.

Statistical analysis

Results were expressed as means ± SE from 4 independent experiments. Student T tests were used for significance of difference between control and treated groups. Statistical significance was considered at $P < 0.05$. The arbitrary densitometry units (AU) were represented for expression.

Results

Effect of NaHS and 5′-AZA on NMDA-R1

Protein and mRNA expression of NMDA-R1 was significantly up regulated in the presence of 100μM Hcy treated cell. Hcy induced up regulation of NMDA-R1 was restored by 30μM NaHS treatment. However, no change was observed in 5μM Hcy, 30μm NaHS and H_2O_2 alone (Fig. 1A–1D).

In order to check the involvement of epigenetic mechanism; we tested the expression of NMDA-R1 with 100μM 5′-AZA (DNMT inhibitor) treatment. 5′-AZA and NaHS treatment significantly decrease the NMDA-R1 protein/mRNA expression in 100 μM Hcy treated cells as compared to control (Fig. 2A–2D). However, no change observed in 5′-AZA and NaHS alone treatments. Effect of 5′-AZA was similar to NaHS treatment over the regulation of NMDA-R1 levels (Fig. 2A–2D).

Effect of NaHS on epigenetic alternation (DNMT1, DNMT3a and DNMT3b)

100μMHcy treatment significantly increased the expression of DNMT1, DNMT3a and decreased the DNMT3b in bEND3 cell indicates increased DNA methylation i.e. epigenetic alternation occurs during HHcy in bEND3 cell. Further treatment with 30μM NaHS restored DNMT1 and DNMT3a expression in 100 μMHcy treated cell in a similar pattern. On the other hand, DNMT3b expression was decreased in 100μM Hcy treated cell which was significantly restored by 30μM NaHS treatment. However, there were no changes observed with NaHS and H_2O_2 alone treatment. These results suggest protective effect of H_2S through epigenetic mechanism (Fig. 3A–B).

Effect of NaHS on Intra cellular Calcium

Calcium level was significantly increased in 100μM Hcy treated cells as compared to control. NaHS treatment significantly restored the calcium level in 100μM Hcy treated cells. However, there was no significant change observed in NaHS and H_2O_2 alone treatment. These results suggest that elevated calcium ion infers close association with alerted mitochondrial function and excitotoxic cell death (Fig. 4A).

Effect of NaHS on total Nitrite estimation

To elucidate the role of NaHS in NO bio-availability, the we measured NO metabolite nitrite levels in cell culture media. Nitrite level was decreased in 100μM Hcy treated cells as compared to control. Treatment with NaHS significantly restored the nitrite level in cells which was co-treated with 100μM Hcy. However, no significant change observed in NaHS alone and 5μMHcy treatment. These results suggested protective effect of H_2S on alerted endothelial function and nitrosative stress during HHcy (Fig. 4B).

Effect of NaHS on redox enzyme levels

To determine the protective role of hydrogen sulfide on Hcy induced imbalance between the redox enzymes, we examined the NOX-4 and SOD-2 protein/mRNA levels by Western blot/ RTPCR analysis. We found significant increase in NOX-4 and decrease in SOD-2 mRNA/ protein levels in 100μM Hcy treated cells. Interestingly, the treatment with NaHS enhanced these effects compared with control. However, no changes were observed in 5μM Hcy, H_2O_2 and NaHS alone treated cells (Fig. 5A–D).

To validate the role of endogenous H_2S in redox stress pre-treated the bEND3 cells with PG (inhibitor of CSE) and we found decreased protein expression of CSE enzyme and increased protein expression of NOX-4 in 100μM Hcy treated cells as compared to control. PG treatment significantly decreased the protein expression of CSE enzyme and increased the protein expression of NOX-4. Treatment with 30μM NaHS ameliorates these effects (Fig. 6A–6B).

To verify the role of NMDA-R1 in redox stress, treat the bEnd3 cells with siRNA of NMDA-R1. Inhibition of NMDA-R1 mitigates the over expression of NOX-4, a major protein involved in mitochondrial oxidative stress. However, NaHS +siRNA not showed any alteration in NOX-4 protein level (Fig. 6C–6D).

These results signify that H_2S and NMDA-R1 plays an important role in Hcy changed the NADPH system of electron transport chain which leads to mitochondrial dysfunction.

NaHS attenuated Hcy-induced intracellular ROS generation

Because the cytotoxicity of Hcy in cells is known to be mediated mainly by oxidative stress, we investigated whether NaHS affects intracellular ROS formation by high Hcy using DCFH-DA fluorescence. Confocal microscopy images showed a significant increase in DCFH-DA fluorescence in 100μM Hcy treated cells in comparison to control cells (Fig. 7B). However, when cells were treated with both 100μM Hcy+30 μM NaHS, DCFH-DA fluorescence was decreased (Fig. 7D). This suggested that Hcy induced intracellular ROS

accumulation was attenuated by hydrogen sulfide. Cells treated with NaHS alone showed weak DCFH-DA fluorescence (Fig. 7D), similar to control cell (Fig. 7A).

Effect of NaHS on mitochondrial oxidant stress

To confirm the generation of oxidative stress in the mitochondrial during high Hcy, cells were loaded with Mito-Sox Red, a cationic probe that distributes to the mitochondrial matrix (Fig. 8). We found a significant increase in mitochondrial super-oxide generation in 100uMHcy treated cells as compared to control but this response was significantly attenuated by NaHS treatment. Interestingly, knock down of NMDA-R1 also mitigated the Hcy-induced increase in mitochondrial superoxide production. Concurrently inhibition of CSE enzyme leads to increase in mitochondrial super-oxide generation. The observed data clearly proved our hypothesis that knock down of NMDA-R1 and inhibition of endogenous H2S production leads to mitochondrial toxicity. This impairment was significantly protected by NaHS treatment (Fig. 8A – 8K).

Effect of NaHS on mitochondrial membrane potential

We want to examine the mechanisms of action behind NaHS protection against high Hcy induced mitochondrial dysfunction; bEND3 cells were examined for mitochondrial oxidative stress, mitochondrial integrity, using dual dye JC-1. The fluorescence data displayed in fig. 9, shown significant less binding of JC-1 to 100μM Hcy treated cells as compared to control that indicates the lowered mitochondrial membrane potential ($\Delta\psi m$). On the other hand, 30μM NaHS treatment in combination of Hcy significantly improved JC-1 binding to the cells indicates improved membrane potential (Fig. 9A – 9K). Pre-treatment with siRNA of NMDA-R with 100 μMHcy showed significantly enhanced mitochondrial membrane potential compared to 100μM Hcy alone treated cells. On the other hand PG (Inhibitor of CSE) also decreased the mitochondrial membrane potential. Interestingly, H_2O_2 treatment showed significantly decrease in mitochondrial membrane potential as indicated by JC-1 binding. These observed data suggest that Hcy induced mitochondrial dysfunction.

Effect of NaHS on Mitochondrial dehydrogenase (MTT) activity

Mitochondrial dehydrogenase activity was down-regulated in 100μM Hcy treated cells as compared to control. 30μMNaHS treatment significantly protects mitochondria and improved the mitochondrial dehydrogenase activity. Mitochondrial activity was also decreased in H_2O_2 treated cells (Fig. 10A).

Effect of NaHS on ATP production

ATP level was significantly reduced in 100μM Hcy treated cells and H_2O_2 alone treatment indicates impaired energy metabolism. Further, 30μM NaHS treatment protects the ATP loss in Hcy treated cells. However, no change observed with NaHS alone treatment (Fig. 10B).

Effect of NaHS mitochondrial DNA damage

Hcy treatment led to significant increase in mitochondrial damage as evidenced by increased expression of mitochondrial DNA damage (**M13597/M13361**) in real time PCR analysis.

Further, we observed that NaHS treatment restored the level mitochondrial DNA. NaHS alone had no effect on mitochondrial damage but H_2O_2 alone showed greater extent of mitochondrial damage (Fig. 10C).

Effect of NaHS on autophagy marker

A treatment with 100μM Hcy caused down regulation of p62 mRNA and its protein expression respectively as compared to control. Whereas, no significant change observed in Hcy 5μM treated cells. A significant decrease in p62 mRNA and protein level also observed in H_2O_2 alone treatment while NaHS alone had no any effect on p62 mRNA and protein expression. Interestingly, NaHS treatment significantly normalized the p62 mRNA and protein expression in 100μM Hcy treated cells (Fig. 11A–11D).

LC3-I/II, ATG-3 and ATG-7 protein expression

Our results showed 100uM Hcy leads to increased expression of LC3-I/II and decreased expression of ATG-3 and ATG-7. Treatment with30uM NaHS significantly ameliorates the altered expression of LC3-I/II, ATG-3 and ATG-7. Further, NaHS alone had no any effect on LC3-I/II, ATG-3 and ATG-7 expression. On the other hand H_2O_2 alone treatment had no effect on LC3-I/II expression but decreased the expression of ATG-3 and ATG-7 (Fig. 11E–11G).

These results suggested that protective effects of NaHS are associated with the anti-autophagic effect during HHcy condition.

NaHS attenuated Hcy induced autophagy in bEND3 Cells

To evaluate whether the cell death caused by Hcy treatment was mediated by autophagy, we examined formation of autophagic vacuoles under a phase contrast microscope by monodansylcadaverine (MDC) staining. As shown in Fig. 12, 100μM Hcy treatment induced the formation of autophagic vacuoles, while co-treatment with 30uM NaHS treatment markedly decreased in autophagic vacuoles production induced by the Hcy treatment. While, in *per se* treatment of NAHS (30μM) hardly induced any formation of autophagic vacuoles. In addition, the amount of autophagic vacuole formation was significantly elevated in H_2O_2 (positive control) treatment as compared to control (Fig 12A–12F).

Effect of NaHS on Endothelial NOS (eNOS) and ET-1 mRNA/Protein Expression

In order to assess the effect of mitochondrial toxicity on endothelial cell function we measured different endothelial markers and effect of NaHS. treatment on it. Our results show that 100μM Hcy decreased the mRNA/protein expression of eNOS and ET-1 as compared to control. However, 30uM NaHS treatment restored eNOS and ET-1 mRNA level in co-treated cells with 100μM Hcy treated cells. However, No significant change was observed in 5μM Hcy, NaHS and H_2O_2 alone treatment (Fig 13A–13D).

Endothelial markers: VE cadherin and CD31

A significant decrease in VE Cadherin and CD31 protein expression was observed in 100μM Hcy treated cells as compared to control. Additionally, NaHS treatment significantly restored the proteins of VE Cadherin and CD31 in 100μM Hcy treated cells (Fig. 13E–13F).

Discussion

The present study demonstrates that neuroprotective role of NaHS (H_2S donor) in HHcy induced mitochondrial-endothelial toxicity. Pathologically high levels of Hcy (100uM) triggered redox-nito- stress leading to mitochondrial toxicity in part by endothelial dysfunction via NMDA-R1 activation. The activation of NMDA-R1 induced mitochondrial oxidative stress and Ca^{2+} influx induces mitochondrial dysfunction and leads to cell death (Moshal et al., 2009). Here, we are presenting the data which is showing HHcy induced mitochondrial-endothelial toxicity and protective mechanism of NaHS (H_2S donor; a gaseous molecule). Therefore, we investigated the effect of NaHS as a therapeutic agent over pathological condition induced by Hcy.

In the present study, we first observed the NMDA-R1 expression in different treated groups. We found that Hcy increased NMDA-R1 expression in the endothelial cells which was ameliorated by NaHS treatment. This observation clearly indicates the antagonizing effect of NaHS over NMDA-R-1. However, no change observed in NMDA-R1 level with NaHS treatment alone that signifies that H_2S actively participated in pathological condition induced by NMDA activation. Further, to check the involvement of epigenetic regulation of NMDA-R1 expression and their correlation with DNA methylation, we employed the 5-Aza (DNMT inhibitor) treatment in Hcy treated cells. Further we also checked the effect of 5-Aza on Hcy induced NMDA-R1 expression. Interestingly, we observed same pattern of NMDA-R1 inhibition as with H_2S.

Recent evidence suggests that the pathogenesis of HHcy in human disease relies on altered epigenetic mechanisms (Kalani et al., 2013, Low et al., 2012). Considering the central role of DNMT1 in the maintenance of DNA methylation, it has been suggested that over expression of this enzyme results in an aberrant function of genes. According to our hypothesis, Hcy induced NMDA-R activation may be associated with epigenetic changes in DNA methylation which leads to endothelial cell toxicity and protective mechanism of H_2S is also mediated through epigenetic changes. Therefore, we examine the effect of 5-Aza and NaHS on DNA methyl transferase gene. Interestingly, we found that NaHS treatment restored the DNMT (DNMT1 DNMT3a, DNMT3b) expression in 100μM Hcy treated cells. In the present study, we also examine the molecular mechanism and link between the NMDA-R1, mitochondrial toxicity, and epigenetic changes in HHcy condition in bEND3 cells. Our present study showed that NaHS significantly mitigates Hcy induced NMDA-R1 and epigenetic changes in a similar fashion of 5-Aza. Finally, we concluded that H_2S may have a protective mechanism through epigenetic changes.

NMDA-R activation might play an important role in regulation of excitotoxicity (Lu et al., 2007) of mammalian brains in several types of neurotoxicity and other type of cell toxicity (Nicholls et al., 2007) and mainly involving NMDA-R. Disrupted Ca^{2+} homeostasis and

recruitment of reactive oxygen/nitrogen species (ROS/RNS) leads to oxidative/nitrosative stress through NMDA-R activation (Sas et al., 2007). Our present data suggests that NaHS mitigates Hcy induced elevated levels of Ca^{2+}, which indicates its protective effect against excitotoxicity and prevents endothelial cell function.

Our previous report suggested that Hcy lead to cellular oxidative stress through formation of reactive oxygen species (ROS), including superoxide anion H_2O_2 (Tyagi et al., 2006)]. The studies have also shown that ROS and Ca^{2+} regulation is tightly bound and disruption of either could affect the other (Petrosillo et al., 2004, Swarnkar et al., 2013). Data of the present study shows that the NaHS treatment prevents the ROS generation in Hcy treated cells and protect from this negative effect. Further, we thought that these excessive Ca^{2+} accumulations and increased free radicals may damage the phospholipid asymmetries which permeabilize the mitochondrial membrane. Therefore, we examined the mitochondrial membrane potential and found decreased membrane potential in Hcy treated cells. Decreased surface membrane potential of mitochondria affects the action potential. Depolarization changes the potential and may result in inhibition of action potential. Prolonged depolarization leads to opening of channels and prevents repolarization thus disturbing mitochondrial ion exchange function. Further, treatment with NaHS significantly maintained decreased mitochondrial membrane potential and thus the integrity and function of mitochondria.

Moreover, H_2O_2 treatment also decreased mitochondrial membrane potential which indicates that free radicals disturb the mitochondrial membrane potential of cells and in later stage causes endothelial cell toxicity. Our present study and previous study also clearly indicates that excessive oxidative damage of mitochondria and cell contributes to a wide range of human pathologies like cerebrovascular diseases and neurodegenerative disorders (Tyagi et al., 2010, Moshal et al., 2008).

In order to demonstrate the role of NMDA-R1 and H_2S on mitochondrial toxicity, we silenced the NMDA receptor with NMDA-R siRNA and inhibited the endogenous H_2S producing enzyme CSE with propargylglycine (PG). We observed lowered mitochondrial toxicity in NMDA-R siRNA treated cells and increased mitochondrial toxicity in PG treated cells as compared to Hcy and control. Mitochondrial toxicity was confirmed by assessment of mitochondrial superoxide generation and mitochondrial membrane potential. Interestingly, NaHS treatment improved the mitochondrial toxicity and mitochondrial membrane potential. Results also confirmed that NMDA-R, NOX-4 over expression and CSE down regulation in Hcy treated cell caused mitochondrial toxicity.

In above observation we have shown that HHcy induced ROS production, as well as disturbed mitochondrial membrane potential which indicates the state of oxidative stress. This altered homeostasis of cell may promote impairment in energy metabolism. In the present study, we noted that Hcy treatment caused impairment in energy as we found decreased ATP level. NaHS treatment restored the ATP level which signifies that this molecule has maintenance properties over energy metabolism. Reduced supply of ATP limits optimal cellular and physiological functions (Shigenaga et al., 1994, Zeevalk et al., 1998). Thus, H_2S could be beneficial for maintenance of energy metabolism of cells. In the

alter experiment we also examined the bioenergetics behavior of cells by succinate dehydrogenase activity (SDH) estimation and observed that H_2S had a repairing mechanism over the bioenergetics behavior of cells. This observed data indicates that H_2S has a protective effect on mitochondrial abrupt function.

In mitochondria, H_2S acts as a cytoprotective factor by inhibiting the activity of cytochrome oxidase by the up regulation of superoxide dismutase (SOD) (Tyagi et al., 2006, 2009, 2010), and it has been reported that diminished enzymatic activity of mitochondrial SOD2 is indicative of oxidative stress (Tyagi et al., 2006). In the present study, we found that NaHS ameliorates decreased expression of SOD2 in Hcy treated cells and maintains proper SOD2 level.

Superoxide production is a requisite event in the excitotoxic cell death process triggered by NMDA-R activation (Girouard et al., 2009), which is a major source of oxidative stress in brain ischemia and other neurological disorders (Girouard et al., 2009). In concurrent with above reports we also found increased expression of the NADPH oxidase (NOX) which triggers the free radicals generation. Our observation indicated that along with H_2S having anti-oxidative properties and anti mito-toxic properties, it also maintained the NADPH level.

Mitochondria are a significant contributor for the generation of endogenous ROS. It is likely that mitochondrial DNA (mtDNA) is susceptible to damage from endogenous ROS and their repair mechanisms are necessary (Tyagi et al., 2006). mtDNA damage could be one of the factors for mitochondrial dysfunction. In the present study, we observed significant mitochondrial DNA damage by HHcy as evidenced from real time PCR analysis. Further, we found that NaHS significantly protected the mtDNA damage. This observation clearly indicates the potential role of H_2S for maintenance of genetic makeup and mitochondrial function.

From the previous and present reports it seems that alteration in mitochondrial activity, mitochondrial membrane potential, mitochondrial superoxide production, mitochondrial DNA damage, and calcium overload are indicators of mitochondrial toxicity and state of dysfunctional mitochondria. Our previous study also support the HHcy induces intracellular reactive oxygen species (ROS) production that leads to the loss of transmembrane mitochondrial membrane potential (accompanied by the release of cytochrome-c from mitochondria and induced apoptosis (Tyagi et al., 2006, 2009). These abnormal functions of mitochondria promote endothelial cell toxicity and alter the redox state of mitochondria. So, we next executed the effect of NaHS on autophagy process and endothelial cell function.

Mitophagy pathways account for degradation of mitochondrial proteins and the function of mitochondria and population is maintained through mitophagy, a form of autophagy (Baker et al., 2013; Zhang et al., 2009). Previously we have shown that autophagy is an important process in the pathogenesis of vascular diseases. NMDA-R1 is a receptor for homocysteine (Hcy) and plays a key role in vascular dysfunction, in part by activating NMDA-R1 involves in vascular disease (Tyagi et al., 2010). Now we are focusing on how mitophagy is involved in endothelial cell toxicity. We examine the LC3, LC3I/II, Atg-3, Atg-7 and p62, markers of autophagy (Moscat and Diaz-Meco, 2009; Johansen and Lamark, 2011). In this study data

showed that NaHS prevents increased LC3, LC3I/II expression and decreased Atg-3, Atg-7, p62 expression in Hcy treated cells which indicate protective effect of H_2S over mitochondrial maintenance. Lysosomal activity, which is actively engaged in autophagy process, was detected with monodansylcadaverine (MDC) staining and we predicted that NaHS minimized increase lysosomal activity as revealed by MDC staining as compared to control.

After we found altered mitochondrial function and autophagy along with severity of oxidative stress, we checked the effect of NaHS on endothelial function. Endothelial nitric oxide synthase (eNOS) plays an important role in vascular permeability, leukocyte extravasation and angiogenesis (Edirimanne et al., 2007). Ours and others previous studies suggested that high levels of Hcy promote oxidative stress in endothelial cells as a result of production of reactive oxygen species (Chambers et al., 1999), which impairs the endothelial function (Eberhardt et al., 2000). In the present study we found that NaHS prevents decreased protein and mRNA expression of eNOS expression along with decreased NO bioavailability and moreover the eNOS expression in Hcy treated cells. Moreover, eNOS level was also altered in H_2O_2 treatment. The outcome of results indicates that decreased expression of eNOS may be mediated by high NMDA-R1 expression and that NaHS maintains eNOS level by antagonizing NMDA-R1. Additionally, data indicates that H_2S maintained the expression of eNOS and NO bioavailability.

ET-1 plays a key role in the development of endothelial dysfunction. ET-1 activates NADPH oxidases and decreases NO bioavailability either by decreasing eNOS via ROS generation (Iglarz and Clozel, 2007; Dammanahalli et al., 2008). Our study showed that NaHS treatment in cells maintains endothelial function by the up regulation of ET-1 expression which correlates with decreased NO bioavailability. It seems that decreased ET-1 expression and eNOS expression are more closely associated with endothelial cell toxicity and dysfunction. Zhen et al. (2012) also reported that elevated plasma ET-1 levels have been directly associated with endothelial dysfunction.

VE-cadherin is a major component of adherens junctions protein is endothelial specific marker and various agents induce a decrease in their expression which alter function of endothelial cells (Bazzoni and Dejana, 2004; Shen et al. 2011; Aslam et al. 2012). Concurrent with this study our study also showed the decreased expression of VE-cadherin in Hcy treated group indicates the Hcy induces vascular-endothelial cell impairment. Moreover, H_2O_2 treatment also showed decreased expression of VE-cadherin which indicates that Hcy might be affecting VE-cadherin expression through free radicals generation mediated by NMDA-R. Further, NaHS treatment ameliorates the VE-cadherin impairment. CD31, an integral membrane glycoprotein and a marker of endothelial cells, plays an important role in maintaining the function of endothelial cells and their altered function associated with cerebrovascular pathology (Luo et al., 2012). In the present study our data showed that Hcy treatment lowered the expression of CD31 which was ameliorated by NaHS treatment. Thus result from the above studies signifies that alerted bEND3 function is properly maintained by H_2S.

In conclusion, present study clearly indicates the protective and potential therapeutic effect of NaHS against HHcy induced mitochondrial toxicity and endothelial dysfunction in bEND3 cells.

Acknowledgments

Contract grant sponsor: NIH

Contract grant numbers: HL107640 NT.

This work was supported by National Institutes of Health grants HL107640-NT.

Abbreviations

Hcy	Homocysteine
HHcy	Hyperhomocysteinemia
H_2S	Hydrogen Sulfide
bEnd.3	Mouse brain endothelial cells
DNMT	DNA methyl transferase
NMDA-R1	NMDA receptor
NaHS	Sodium hydrogen sulphide
ROS	Reactive oxygen species
NO	Nitric oxide
NOX-4	NADPH oxidase-4
SOD2	Super oxide dismutase
eNOS	Endothelial nitric oxide synthase
ET-1	Endothelin-1
VE- Cadherin	Vascular endothelial Cadherin
PBS	Phosphate buffer saline
5′-aza	5′-azacitidine
ATP	Adenosine triphosphate
LC3	Microtubule-associated protein -light chain 3I/II
Atg3/7	autophagy-related gene3/7
PG	DL –Propargylglycine

References

1. Aslam M, Pfeil U, Gunduz D, Rafiq A, Kummer W, Piper HM, et al. Intermedin (adrenomedullin2) stabilizes the endothelial barrier and antagonizes thrombin-induced barrier failure in endothelial cell monolayers. Br J Pharmacol. 2011; 165:208–22. [PubMed: 21671901]

2. Austin RC, Lentz SR, Werstuck GH. Role of hyperhomocysteinemia in endothelial dysfunction and atherothrombotic disease. Cell Death Differ. 2004; 11 (Suppl 1):S56–64. [PubMed: 15243582]
3. Baker MJ, Tatsuta T, Langer T. Quality control of mitochondrial proteostasis. Cold Spring Harb Perspect Biol. 2013:3.
4. Bazzoni G, Dejana E. Endothelial cell-to-cell junctions: molecular organization and role in vascular homeostasis. Physiol Rev. 2004; 84:869–901. [PubMed: 15269339]
5. Chambers JC, McGregor A, Jean-Marie J, Obeid OA, Kooner JS. Demonstration of rapid onset vascular endothelial dysfunction after hyperhomocysteinemia: an effect reversible with vitamin C therapy. Circulation. 1999; 99:1156–60. [PubMed: 10069782]
6. Chang PY, Lu SC, Lee CM, Chen YJ, Dugan TA, Huang WH, et al. Homocysteine inhibits arterial endothelial cell growth through transcriptional downregulation of fibroblast growth factor-2 involving G protein and DNA methylation. Circ Res. 2008; 102:933–41. [PubMed: 18309099]
7. Chen CA, Wang TY, Varadharaj S, Reyes LA, Hemann C, Talukder MA, et al. S-glutathionylation uncouples eNOS and regulates its cellular and vascular function. Nature. 2010; 468:1115–8. [PubMed: 21179168]
8. Cirio MC, Martel J, Mann M, Toppings M, Bartolomei M, Trasler J, et al. DNA methyltransferase 1o functions during preimplantation development to preclude a profound level of epigenetic variation. Dev Biol. 2008; 324:139–50. [PubMed: 18845137]
9. Dammanahalli KJ, Sun Z. Endothelins and NADPH oxidases in the cardiovascular system. Clin Exp Pharmacol Physiol. 2008; 35:2–6. [PubMed: 18047620]
10. Doronzo G, Russo I, Del Mese P, Viretto M, Mattiello L, Trovati M, et al. Role of NMDA receptor in homocysteine-induced activation of mitogen-activated protein kinase and phosphatidyl inositol 3-kinase pathways in cultured human vascular smooth muscle cells. Thromb Res. 2009; 125:e23–32. [PubMed: 19766294]
11. Duchen MR. Roles of mitochondria in health and disease. Diabetes. 2004; 53 (Suppl 1):S96–102. [PubMed: 14749273]
12. Eberhardt RT, Forgione MA, Cap A, Leopold JA, Rudd MA, Trolliet M, et al. Endothelial dysfunction in a murine model of mild hyperhomocyst(e)inemia. J Clin Invest. 2000; 106:483–91. [PubMed: 10953023]
13. Eberhardt W, Huwiler A, Beck KF, Walpen S, Pfeilschifter J. Amplification of IL-1 beta-induced matrix metalloproteinase-9 expression by superoxide in rat glomerular mesangial cells is mediated by increased activities of NF-kappa B and activating protein-1 and involves activation of the mitogen-activated protein kinase pathways. J Immunol. 2000; 165:5788–97. [PubMed: 11067938]
14. Edirimanne VE, Woo CW, Siow YL, Pierce GN, Xie JY, OK. Homocysteine stimulates NADPH oxidase-mediated superoxide production leading to endothelial dysfunction in rats. Can J Physiol Pharmacol. 2007; 85:1236–47. [PubMed: 18066125]
15. Faraci FM, Lentz SR. Hyperhomocysteinemia, oxidative stress, and cerebral vascular dysfunction. Stroke. 2004; 35:345–7. [PubMed: 14757874]
16. Girouard H, Wang G, Gallo EF, Anrather J, Zhou P, Pickel VM, et al. NMDA receptor activation increases free radical production through nitric oxide and NOX2. J Neurosci. 2009; 29:2545–52. [PubMed: 19244529]
17. Green LC, Wagner DA, Glogowski J, Skipper PL, Wishnok JS, Tannenbaum SR. Analysis of nitrate, nitrite, and [15N] nitrate in biological fluids. Anal Biochem. 1982; 126:131–8. [PubMed: 7181105]
18. Grynkiewicz G, Poenie M, Tsien RY. A new generation of Ca2+ indicators with greatly improved fluorescence properties. J Biol Chem. 1985; 260:3440–50. [PubMed: 3838314]
19. Iglarz M, Clozel M. Mechanisms of ET-1-induced endothelial dysfunction. J Cardiovasc Pharmacol. 2007; 50:621–8. [PubMed: 18091577]
20. Johansen T, Lamark T. Selective autophagy mediated by autophagic adapter proteins. Autophagy. 2011; 7:279–96. [PubMed: 21189453]
21. Kalani A, Kamat PK, Givvimani S, Brown K, Metreveli N, Tyagi SC, et al. Nutri-epigenetics Ameliorates Blood-Brain Barrier Damage and Neurodegeneration in Hyperhomocysteinemia: Role of Folic Acid. J Mol Neurosci. 2013; 13:0122–25.

22. Kamat PK, Kalani A, Givvimani S, Sathnur PB, Tyagi SC, Tyagi N. Hydrogen sulfide attenuates neurodegeneration and neurovascular dysfunction induced by intracerebral-administered homocysteine in mice. Neuroscience. 2013; 252:302–19. [PubMed: 23912038]
23. Kamat PK, Tota S, Shukla R, Ali S, Najmi AK, Nath C. Mitochondrial dysfunction: a crucial event in okadaic acid (ICV) induced memory impairment and apoptotic cell death in rat brain. Pharmacol Biochem Behav. 2011; 100:311–9. [PubMed: 21893081]
24. Kimura H. Hydrogen sulfide: its production, release and functions. Amino Acids. 2011; 41:113–121. [PubMed: 20191298]
25. Lalo U, Pankratov Y, Kirchhoff F, North RA, Verkhratsky A. NMDA receptors mediate neuron-to-glia signaling in mouse cortical astrocytes. J Neurosci. 2006; 26:2673–83. [PubMed: 16525046]
26. Levonen AL, Lapatto R, Saksela M, Raivio KO. Human cystathionine gamma-lyase: developmental and in vitro expression of two isoforms. Biochem J. 2000; 347(Pt 1):291–5. [PubMed: 10727430]
27. Lipton SA. Paradigm shift in NMDA receptor antagonist drug development: molecular mechanism of uncompetitive inhibition by memantine in the treatment of Alzheimer's disease and other neurologic disorders. J Alzheimers Dis. 2004; 6:S61–74. [PubMed: 15665416]
28. Low HQ, Chen CP, Kasiman K, Thalamuthu A, Ng SS, Foo JN, et al. A comprehensive association analysis of homocysteine metabolic pathway genes in Singaporean Chinese with ischemic stroke. PLoS One. 2012; 6:e24757. [PubMed: 21935458]
29. Lowicka E, Beltowski J. Hydrogen sulfide (H2S) - the third gas of interest for pharmacologists. Pharmacol Rep. 2007; 59:4–24. [PubMed: 17377202]
30. Lu Y, Rosenberg PA. NMDA receptor-mediated extracellular adenosine accumulation is blocked by phosphatase 1/2A inhibitors. Brain Res. 2007; 1155:116–24. [PubMed: 17509540]
31. Luo C, Li Y, Wang H, Feng Z, Li Y, Long J, et al. Mitochondrial accumulation under oxidative stress is due to defects in autophagy. J Cell Biochem. 2012; 114:212–9. [PubMed: 22903604]
32. Moscat J, Diaz-Meco MT. p62 at the crossroads of autophagy, apoptosis, and cancer. Cell. 2009; 137:1001–4. [PubMed: 19524504]
33. Moshal KS, Kumar M, Tyagi N, Mishra PK, Metreveli N, Rodriguez WE, et al. Restoration of contractility in hyperhomocysteinemia by cardiac-specific deletion of NMDA-R1. Am J Physiol Heart Circ Physiol. 2009; 296:H887–92. [PubMed: 19181966]
34. Moshal KS, Tipparaju SM, Vacek TP, Kumar M, Singh M, Frank IE, et al. Mitochondrial matrix metalloproteinase activation decreases myocyte contractility in hyperhomocysteinemia. Am J Physiol Heart Circ Physiol. 2008; 295:H890–7. [PubMed: 18567713]
35. Nicholls DG, Johnson-Cadwell L, Vesce S, Jekabsons M, Yadava N. Bioenergetics of mitochondria in cultured neurons and their role in glutamate excitotoxicity. J Neurosci Res. 2007; 85:3206–12. [PubMed: 17455297]
36. Obeid R, Herrmann W. Mechanisms of homocysteine neurotoxicity in neurodegenerative diseases with special reference to dementia. FEBS Lett. 2006; 580:2994–3005. [PubMed: 16697371]
37. Petrosillo G, Ruggiero FM, Pistolese M, Paradies G. Ca2+-induced reactive oxygen species production promotes cytochrome c release from rat liver mitochondria via mitochondrial permeability transition (MPT)-dependent and MPT-independent mechanisms: role of cardiolipin. J Biol Chem. 2004; 279:53103–8. [PubMed: 15475362]
38. Poddar R, Paul S. Homocysteine-NMDA receptor-mediated activation of extracellular signal-regulated kinase leads to neuronal cell death. J Neurochem. 2009; 110:1095–106. [PubMed: 19508427]
39. Rai S, Kamat PK, Nath C, Shukla R. A study on neuroinflammation and NMDA receptor function in STZ (ICV) induced memory impaired rats. J Neuroimmunol. 2013; 254:1–9. [PubMed: 23021418]
40. Reinhart B, Chaillet JR. Genomic imprinting: cis-acting sequences and regional control. Int Rev Cytol. 2005; 243:173–213. [PubMed: 15797460]
41. Santos-Reboucas CB, Pimentel MM. Implication of abnormal epigenetic patterns for human diseases. Eur J Hum Genet. 2007; 15:10–7. [PubMed: 17047674]

42. Sas K, Robotka H, Toldi J, Vecsei L. Mitochondria, metabolic disturbances, oxidative stress and the kynurenine system, with focus on neurodegenerative disorders. J Neurol Sci. 2007; 257:221–39. [PubMed: 17462670]
43. Shen WD, Ji Y, Liu PF, Xiang B, Chen GQ, Huang B, et al. Correlation of E-cadherin and CD44v6 expression with clinical pathology in esophageal carcinoma. Mol Med Rep. 2011; 5:817–21. [PubMed: 22139342]
44. Shigenaga MK, Hagen TM, Ames BN. Oxidative damage and mitochondrial decay in aging. Proc Natl Acad Sci U S A. 1994; 91:10771–8. [PubMed: 7971961]
45. Swarnkar S, Goswami P, Kamat PK, Gupta S, Patro IK, Singh S, et al. Rotenone-induced apoptosis and role of calcium: a study on Neuro-2a cells. Arch Toxicol. 2013; 86:1387–97. [PubMed: 22526376]
46. Tyagi N, Gillespie W, Vacek JC, Sen U, Tyagi SC, Lominadze D. Activation of GABA-A receptor ameliorates homocysteine-induced MMP-9 activation by ERK pathway. J Cell Physiol. 2009; 220:257–66. [PubMed: 19308943]
47. Tyagi N, Givvimani S, Qipshidze N, Kundu S, Kapoor S, Vacek JC, et al. Hydrogen sulfide mitigates matrix metalloproteinase-9 activity and neurovascular permeability in hyperhomocysteinemic mice. Neurochem Int. 2010; 56:301–7. [PubMed: 19913585]
48. Tyagi N, Mishra PK, Tyagi SC. Homocysteine, hydrogen sulfide (H2S) and NMDA-receptor in heart failure. Indian J Biochem Biophys. 2009; 46:441–6. [PubMed: 20361707]
49. Tyagi N, Ovechkin AV, Lominadze D, Moshal KS, Tyagi SC. Mitochondrial mechanism of microvascular endothelial cells apoptosis in hyperhomocysteinemia. J Cell Biochem. 2006; 98:1150–62. [PubMed: 16514665]
50. Tyagi N, Sedoris KC, Steed M, Ovechkin AV, Moshal KS, Tyagi SC. Mechanisms of homocysteine-induced oxidative stress. Am J Physiol Heart Circ Physiol. 2005; 289:H2649–56. [PubMed: 16085680]
51. Vazquez CL, Colombo MI. Assays to Assess Autophagy Induction and Fusion of Autophagic Vacuoles with a Degradative Compartment, Using Monodansylcadaverine (MDC) and DQ-BSA. Methods in Enzymology. 2009; 452:85–95. [PubMed: 19200877]
52. Weiss N, Miller F, Cazaubon S, Couraud PO. The blood-brain barrier in brain homeostasis and neurological diseases. Biochim Biophys Acta. 2009; 1788:842–57. [PubMed: 19061857]
53. White JE, Tsan MF. Differential induction of TNF-alpha and MnSOD by endotoxin: role of reactive oxygen species and NADPH oxidase. Am J Respir Cell Mol Biol. 2001; 24:164–9. [PubMed: 11159050]
54. Wilson AS, Power BE, Molloy PL. DNA hypomethylation and human diseases. Biochim Biophys Acta. 2007; 1775:138–62. [PubMed: 17045745]
55. Zeevalk GD, Bernard LP, Sinha C, Ehrhart J, Nicklas WJ. Excitotoxicity and oxidative stress during inhibition of energy metabolism. Dev Neurosci. 1998; 20:444–53. [PubMed: 9778583]
56. Zhang J, Kundu M, Ney PA. Mitophagy in mammalian cells: the reticulocyte model. Methods Enzymol. 2009; 452:227–45. [PubMed: 19200886]
57. Zhen P, Zhao Q, Hou D, Liu T, Jiang D, Duan J, et al. Genistein attenuates vascular endothelial impairment in ovariectomized hyperhomocysteinemic rats. J Biomed Biotechnol. 2012:730462. [PubMed: 23226943]

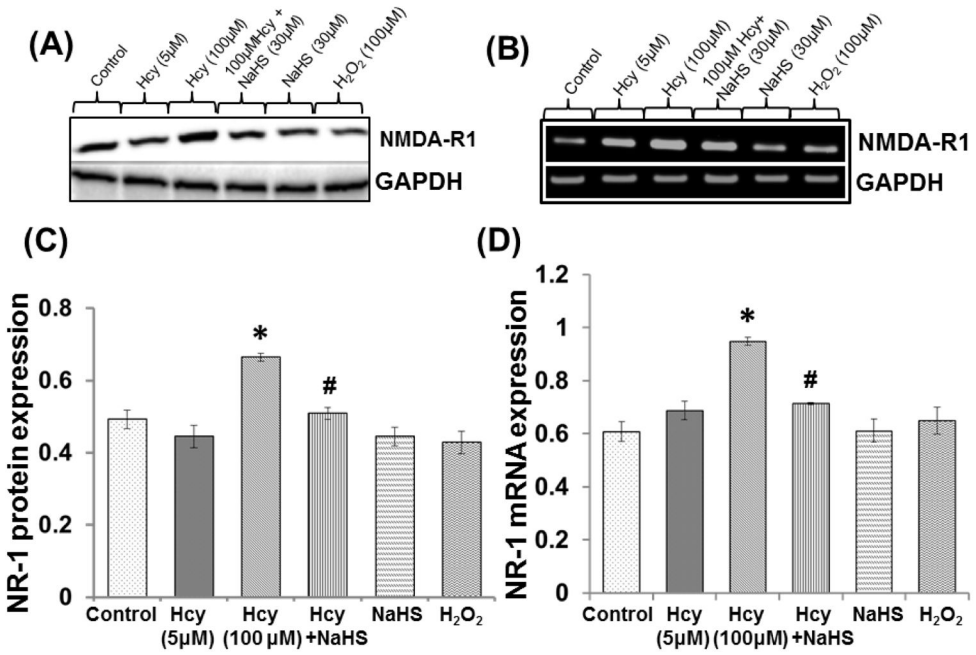

Fig. 1. The effect of NaHS on NMDA receptor

Representative blots and bands showing **(A)** NMDAR-1 protein **(B)** mRNA expression **(C–D)** Densitometric analysis of NMDAR1 protein and mRNA expressions as represented in the bar diagram. GAPDH was used as loading control. Data represents mean ±SE from n = 4 per group; $^{**}P< 0.005$ *vs* control group, $^{\#}P< 0.05$, $^{\#\#}P< 0.001$ *vs* to Hcy treated group.

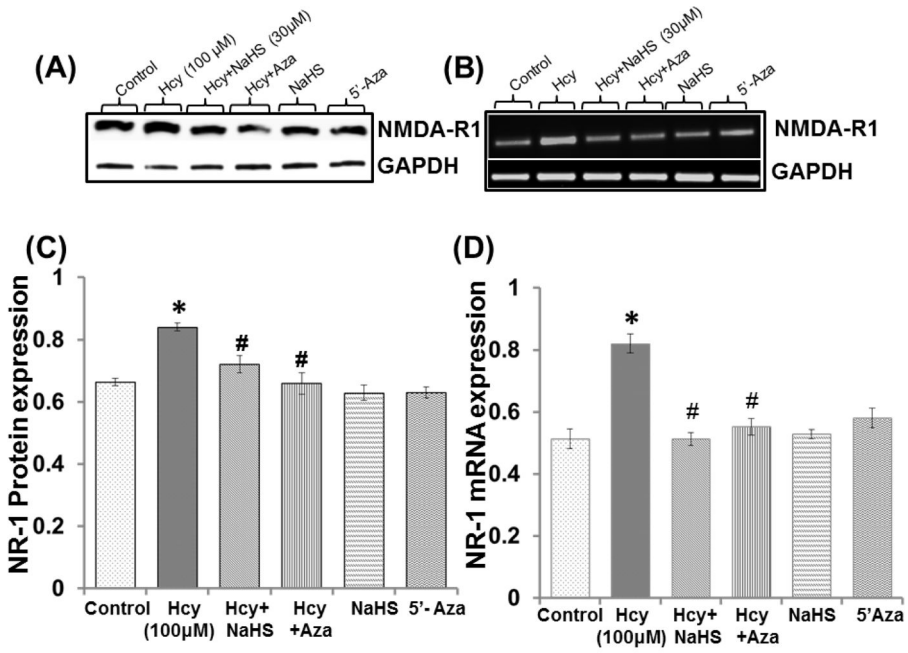

Fig. 2. The effect of NaHS and 5-Azacytidine on Hcy induced NMDA receptor

Western blot and PCR bands showing **(A)** NMDAR-1 protein **(B)** mRNA **(C–D)** Densitometric analysis of NMDAR1 protein and mRNA expressions as represented in the bar diagram. GAPDH was used as loading control. Data represents mean ±SE from n = 4 per group; $^{**}P< 0.005$ *vs* control group, $^{\#}P< 0.05$, $^{\#\#}P< 0.005$ *vs* to Hcy treated group.

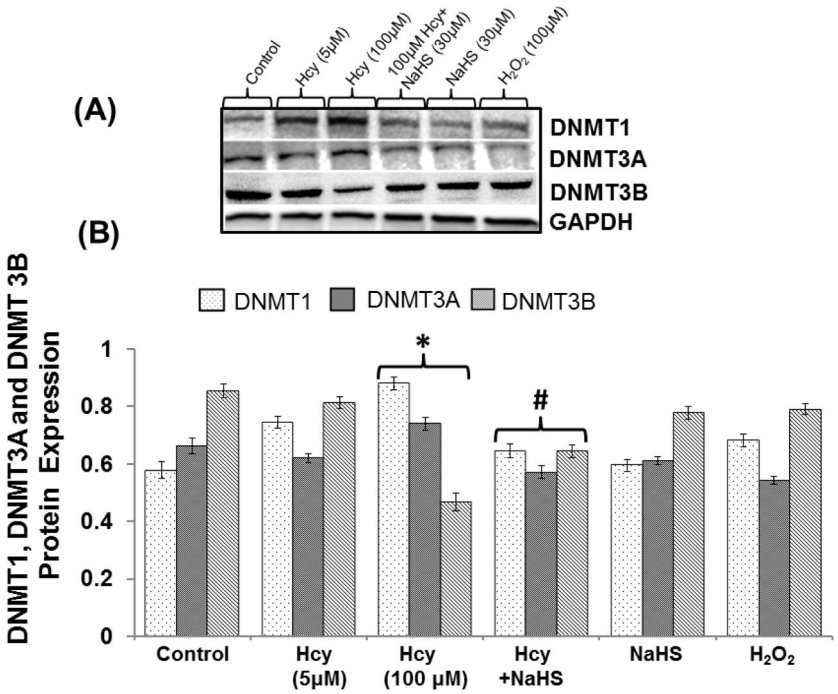

Fig. 3. The effect of NaHS on DNA methylation

(A) Representative Immunoblot probed with anti-DNMTs antibodies (DNMT1, DNMT3a, and DNMT3b) **(B)** Protein expression levels of DNMTs were quantitated and represented as bar graph. Data represents mean ±SE from n = 4 per group; $^{*}P< 0.05$ *vs* control group, $^{\#}P< 0.05$, $^{\#\#\#}P< 0.0001$ *vs* to Hcy treated group.

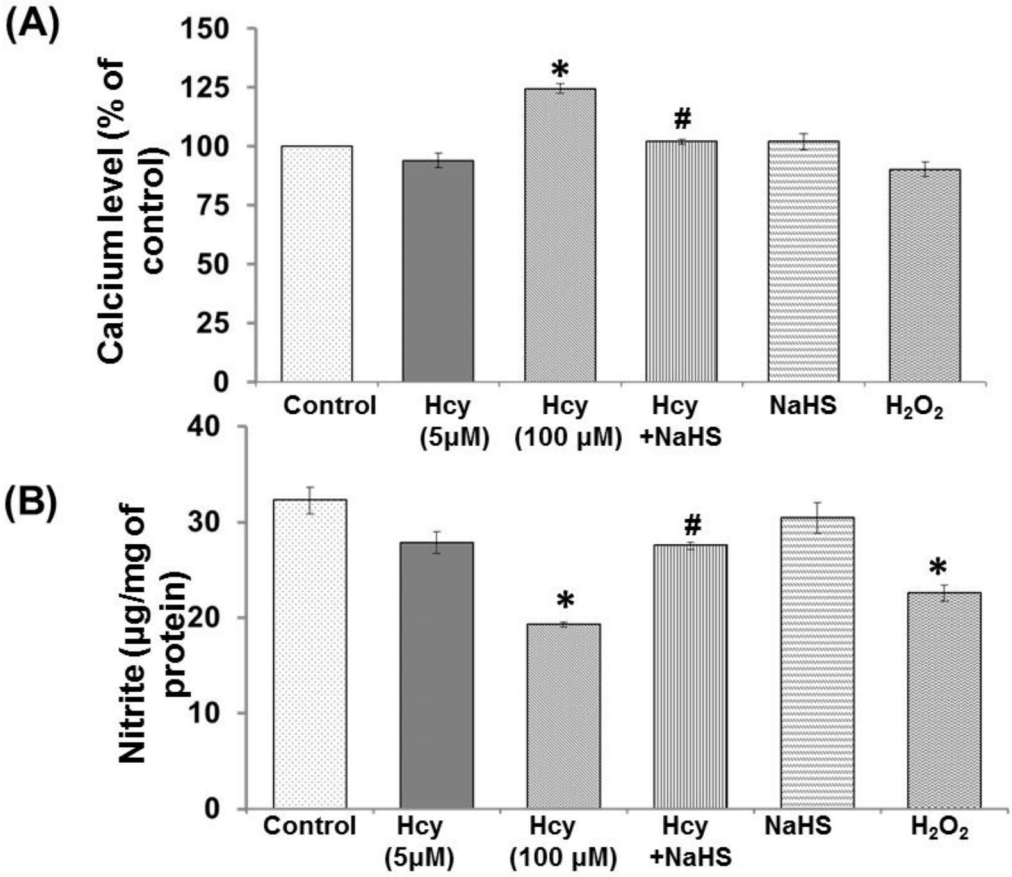

Fig. 4. Protective effect of NaHS on intracellular Ca^{2+} and NO bioavailability

(A) Cells were loaded with Fura 2AM, placed in a spectrofluorometer, as described in experimental procedures. **(B)** Nitrite measurement using fluorometric assay (nmol/mg of protein). Data represents mean ±SE from n = 4 per group; $^{**}P< 0.005$ *vs* control group, $^{\#}P< 0.05$ *vs* to Hcy treated group.

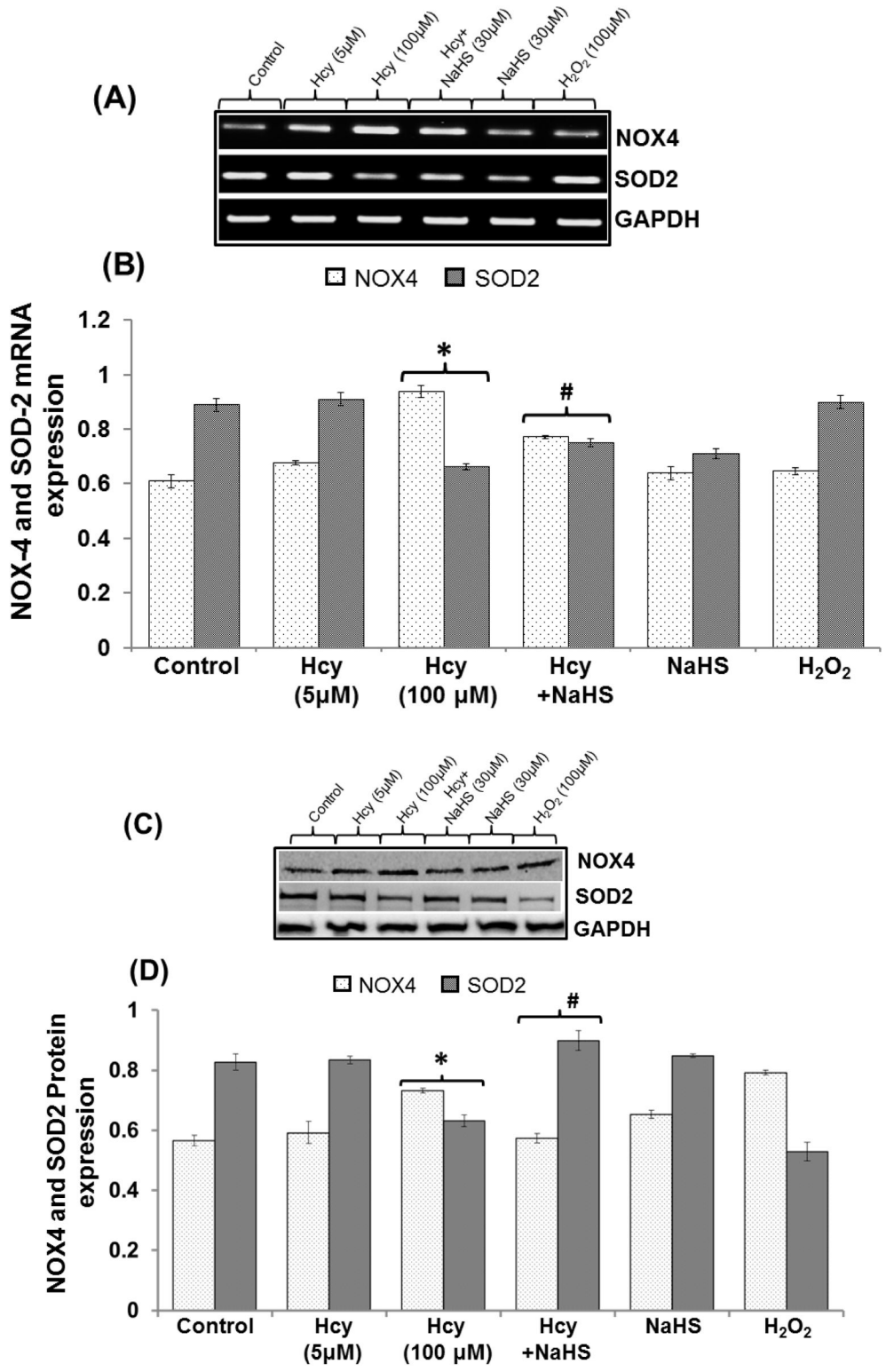

Fig. 5. Protective effect of NaHS on redox stress

(A) Representative Immunoblots for NOX-4, and SOD-2. **(B)** Densitometric analysis of NOX-4 and SOD-2 protein expressions as represented in the bar diagram **(C)** Represented

semi quantitative mRNA expression for NOX-4 and SOD-2 **(D)** Densitometric analysis of NOX-4 and SOD-2 mRNA expressions as represented in the bar diagram. Data represents mean ±SE from n = 4 per group. $^{*}P< 0.05$, $^{**}P< 0.005$ *vs* Control group and $^{\#}P< 0.05$, $^{\#\#}P< 0.001$ *vs* Hcy treated group.

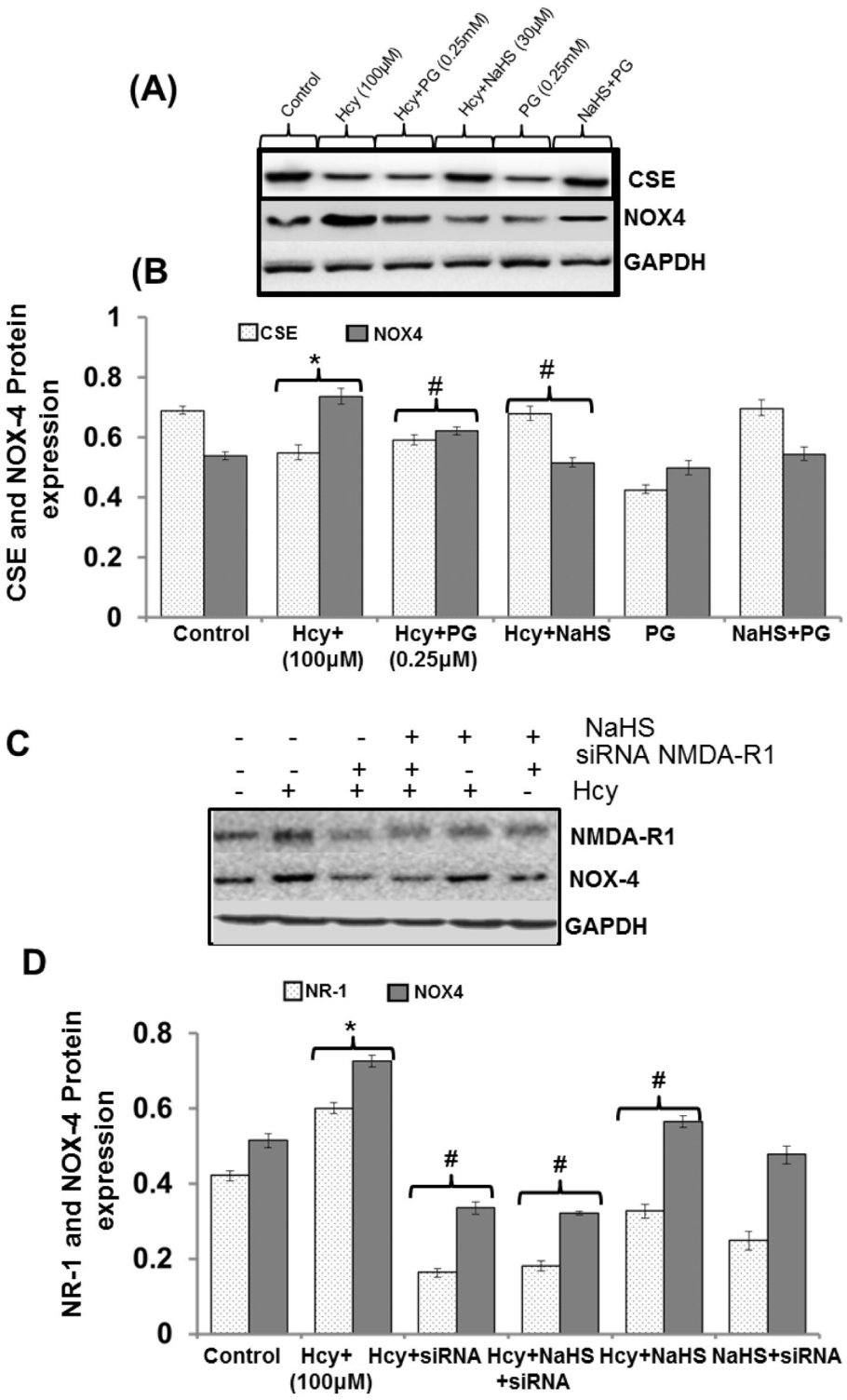

Fig. 6. Effect of siRNA, PG and NaHS on NOX-4, CSE and NMDAR1

(A) Representative Immunoblots for NOX-4, and NMDAR1 and **(B)** Densitometric analysis of NOX-4 and NR1 protein expressions as shown in the bar diagram. Data represents mean ±SE from n = 4 per group. $^{*}P< 0.05$, $^{**}P< 0.005$ *vs* Control group and $^{\#}P< 0.05$, $^{\#\#}P<$

0.001 vs Hcy treated group **(C)** Representative immunoblots for NOX-4, and CSE **(D)** densitometric analysis of NOX-4 and CSE protein expressions as shown in the bar diagram. Data represents mean ±SE from n = 4 per group. $^{*}P < 0.05$, $^{**}P < 0.005$ *vs* Control group and $^{\#}P < 0.05$, $^{\#\#}P < 0.001$ *vs* Hcy treated group.

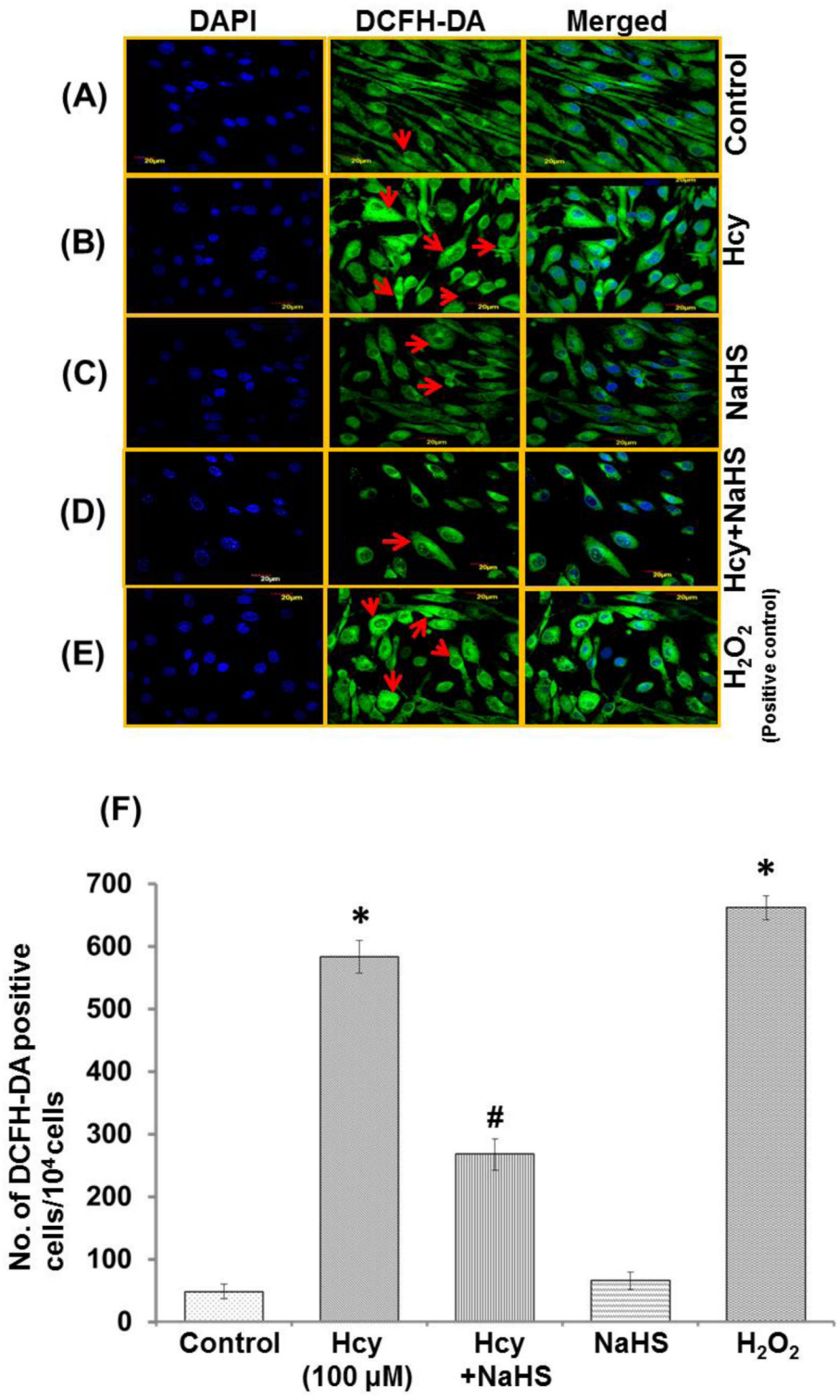

Fig. 7. Effect of NaHS on intracellular ROS generation

(**A**) Control (B) 100μMHcy **(C)** 100μMHcy+30μM NaHS **(D)** 30μM NaHS **(E)** H_2O_2 **(F)** Bar diagram showing ROS generation in arbitrary unit. Data represents mean ±SE from n = 4 per group. $^{***}P < 0.0001$ *vs* Control group and $^{\#\#}P < 0.01$ *vs* Hcy treated group. The arrows

indicate the fluorescence of ROS in the endothelial cell. n = 4 per group. Images were captured at 100X.

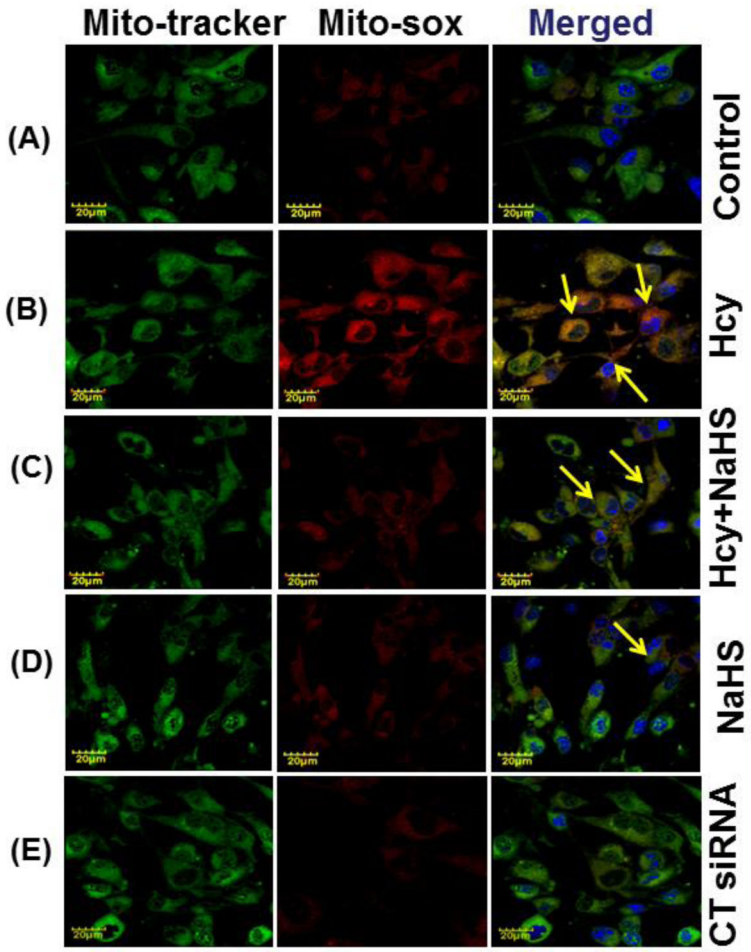

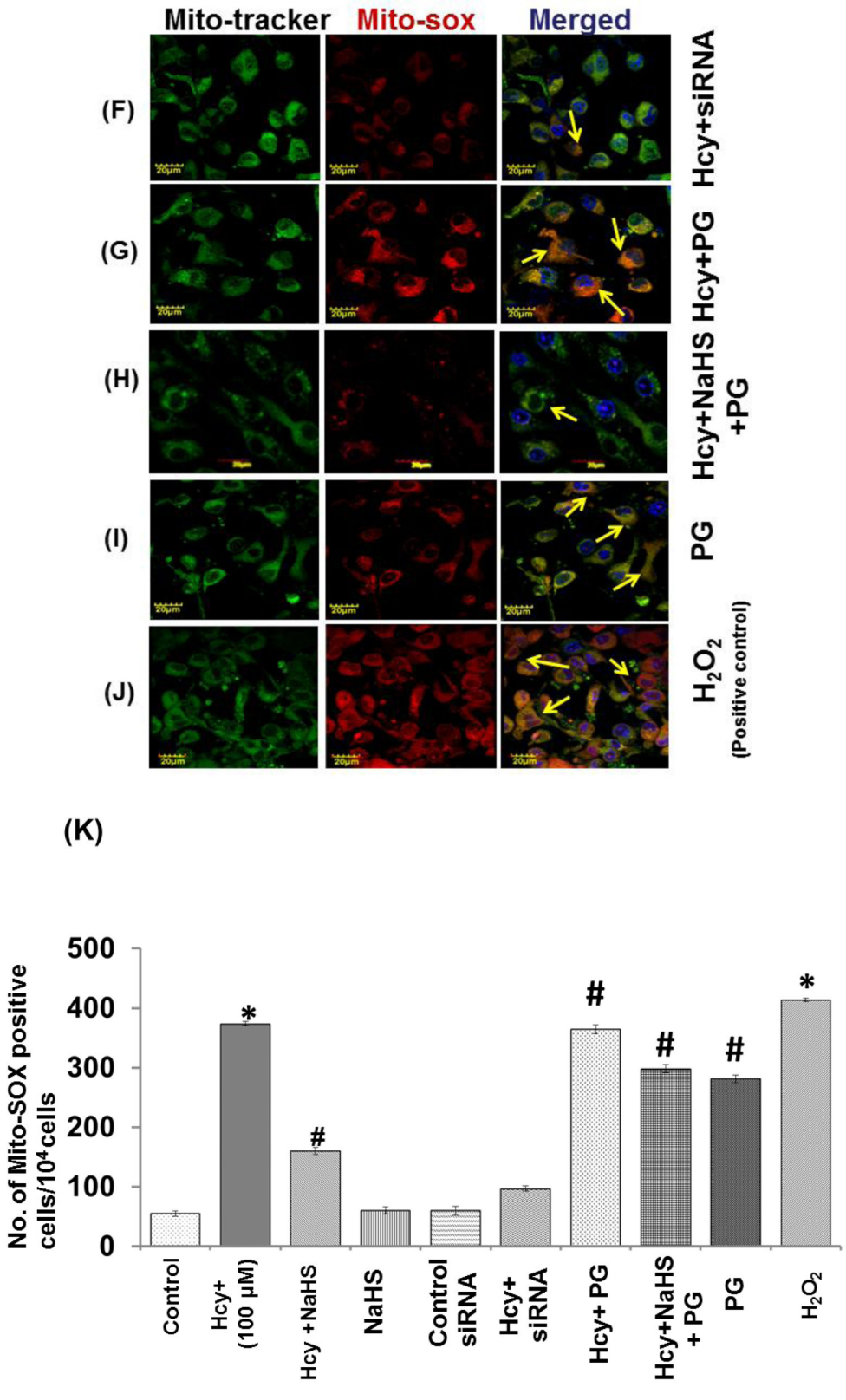

Fig. 8. Effect of NaHS, siRNA and PG on Hcy induced mitochondrial ROS generation

(A) Control cells **(B) 1**00μMHcy **(C)** 100μMHcy+30μM NaHS **(D)** 30μM NaHS (E) Control siRNA group. **(F) 1**00μMHcy+ siRNA **(G)** Hcy+PG and **(H)** Hcy+NaHS+PG **(I)** PG alone **(J)** H_2O_2 treated cells showed significant high ROS generation. Representative bar diagram **(K)** showing ROS generation in different treated group and expressed in arbitrary unit. Data represents mean ±SE from n = 4 per group. $^{***}P< 0.0001$ *vs* Control group and $^{\#\#}P< 0.01$ *vs* Hcy treated group. Images were captured at 100X.

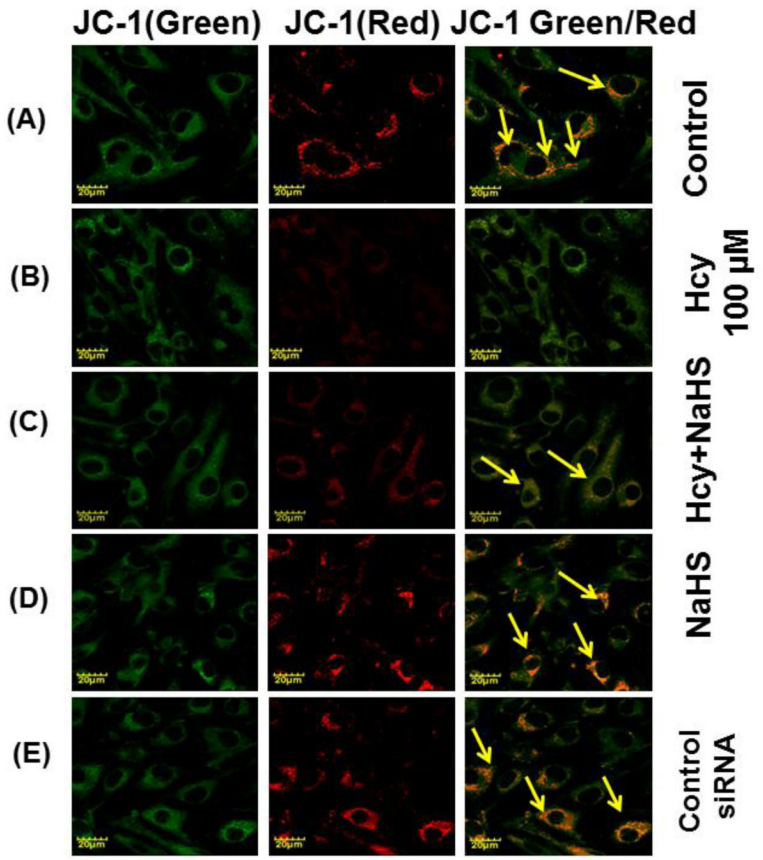

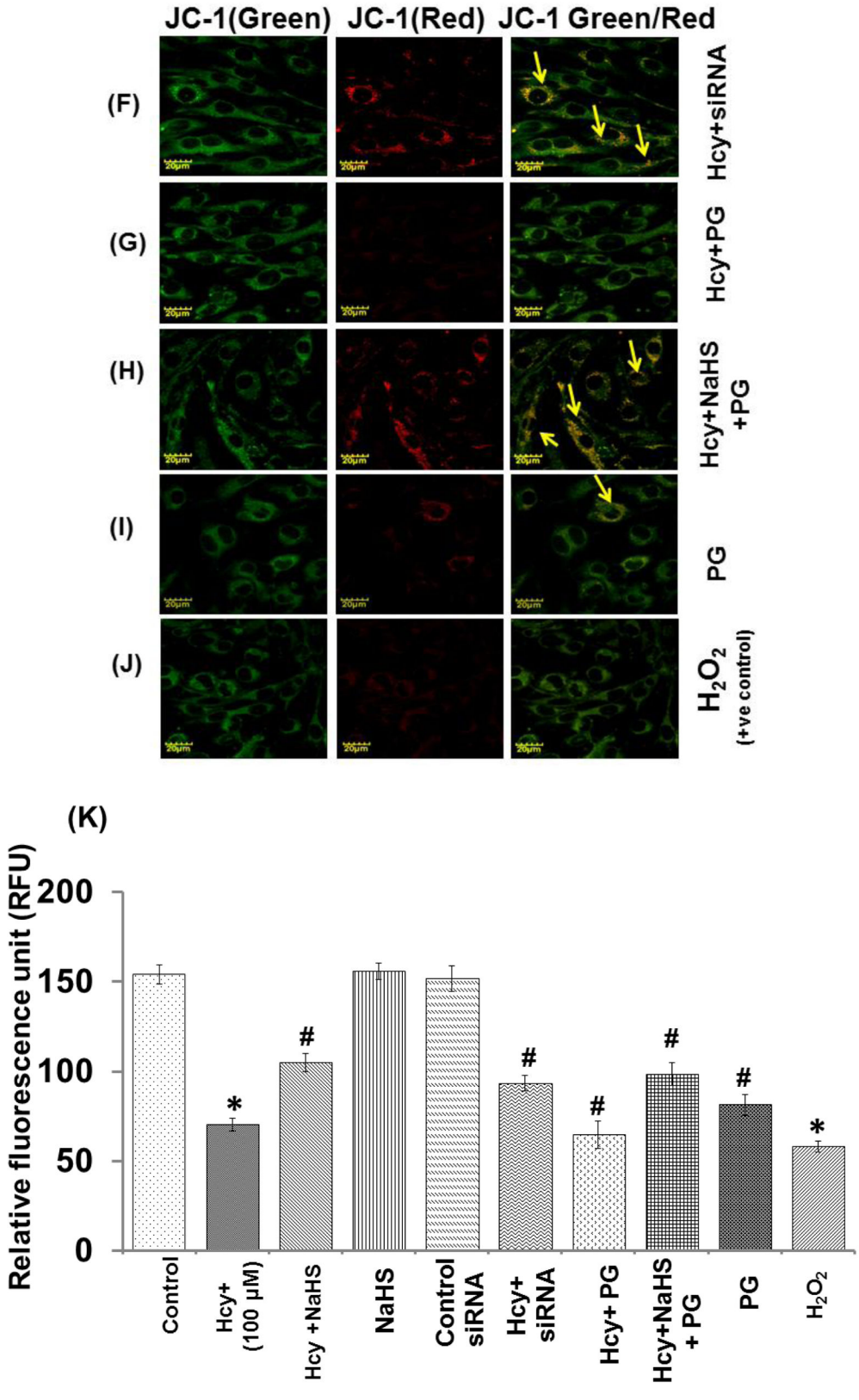

Fig. 9. Confocal microscopy of membrane potential in different treated group

(A) Control cells **(B) 1**00μMHcy **(C)** 100μMHcy+30μM NaHS **(D)** 30μM NaHS **(E)** Control siRNA group. **(F) 1**00μMHcy+ siRNA **(G)** Hcy+PG **(H)** Hcy+NaHS+PG **(I)** PG alone **(J)** H_2O_2 treated cells showed significant high ROS generation. Representative bar diagram **(K)** showing relative fluorescence unit different treated group. Data represents mean ±SE from n = 4 per group. $^{*}P< 0.05$, $^{**}P< 0.005$ *vs* Control group and $^{\#}P< 0.05$, $^{\#\#}P< 0.001$ *vs* Hcy treated group. Images were captured at 100X.

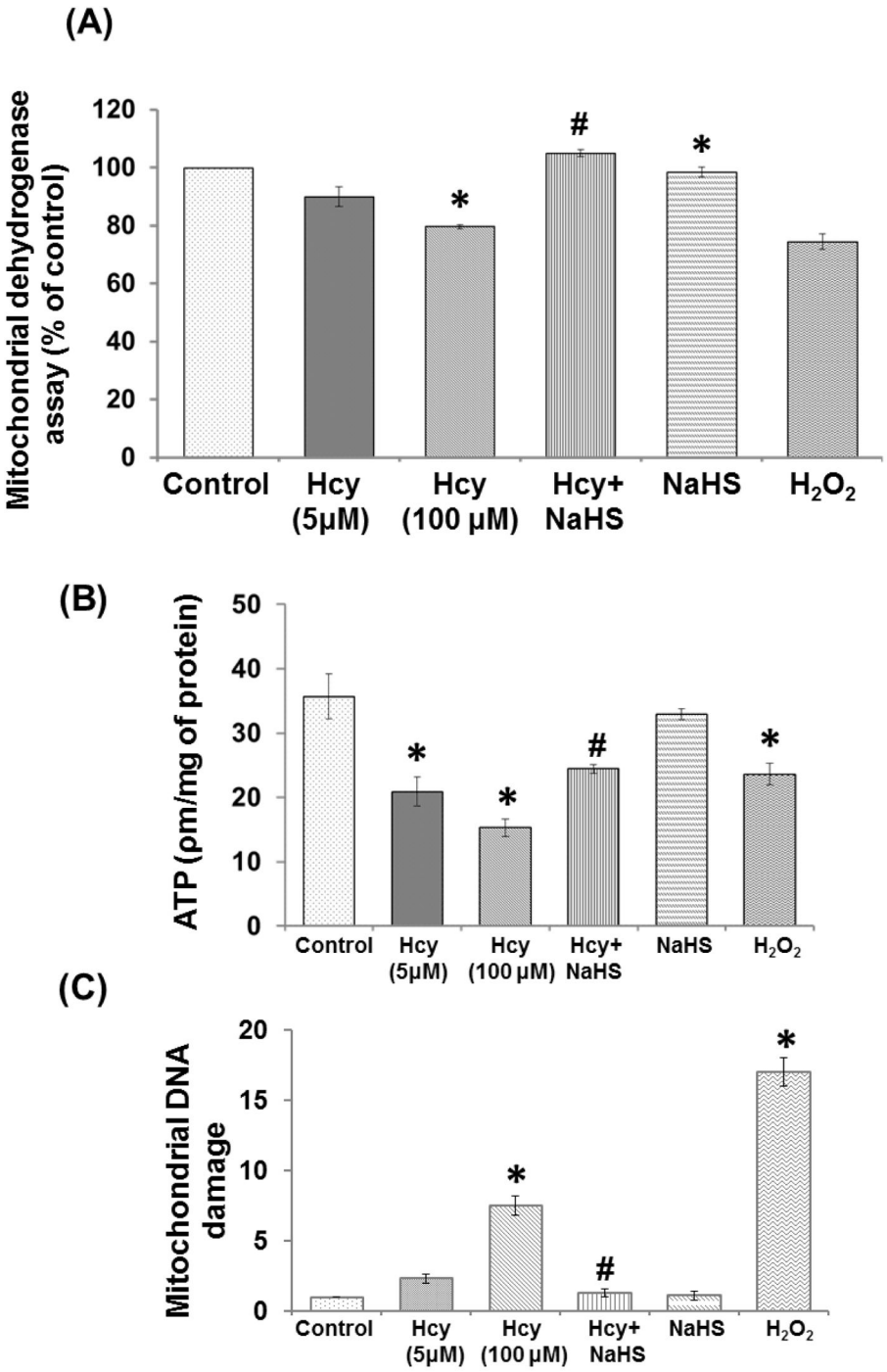

Fig. 10. Exogenous NaHS supplement maintains mitochondrial function

(A) Hcy induced mitochondrial dehydrogenase activity: MTT assay of different group showed that significantly prevents the decreased dehydrogenase activity as revealed from formazan formation. **(B) Hcy induced change in energy metabolism:** Biochemical analysis of ATP from different group indicating H_2S significantly protect the Hcy induced lowered ATP level and H_2S imply mitochondrial protective effect. $^{*}P< 0.05$ *vs* control group *vs* to Hcy treated group). **(C) Mitochondrial DNA damage:** Exogenous NaHS supplement

significantly protect mitochondrial DNA damage. Data represents n=4 group $^{*}P< 0.05$, $^{**}P< 0.005$*vs* control group, $^{\#}P< 0.05$, $^{\#\#}P< 0.005$ *vs* to Hcy treated group.

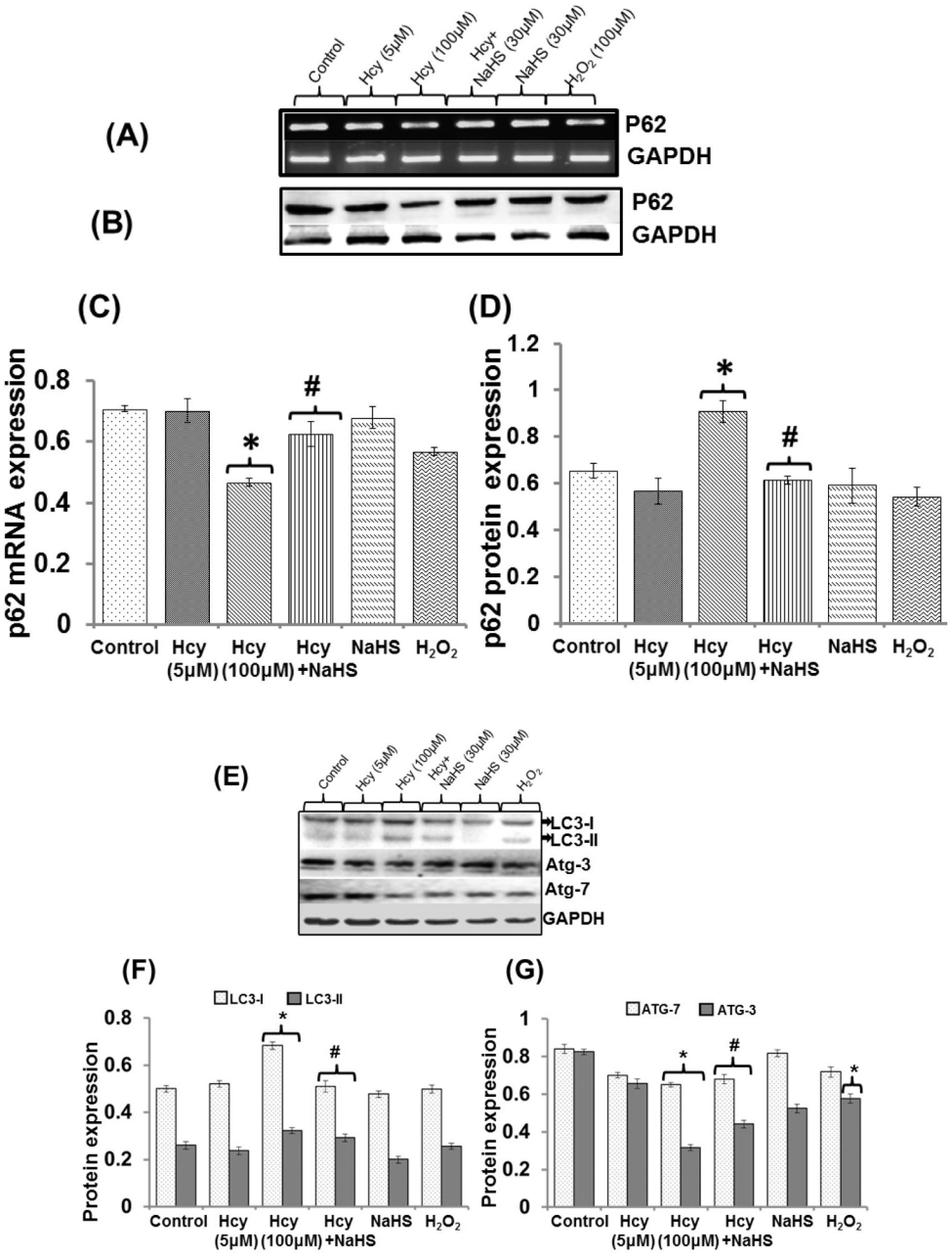

Fig. 11. The effect of NaHS on autophagy

(A) Represents Immunoblot of p62 **(B)** Densitometric analysis of p62 protein expressions as shown in the bar diagram **(C)** Represented semi quantitative mRNA expression for p62 (**D)** Densitometric analysis of p62 mRNA expressions as shown in the bar diagram (**E)** Represents Immunoblot of LC3-I/II Atg-3 and Atg-7 (**F–G)** represents densitometric analysis of LC3-I/II Atg-3 and Atg-7 as shown in the bar diagram. Data represents mean ±SE from n =4 per group. $^{*}P< 0.05$, $^{**}P< 0.005$ *vs* Control group and $^{\#\#}P< 0.001$ *vs* Hcy treated group.

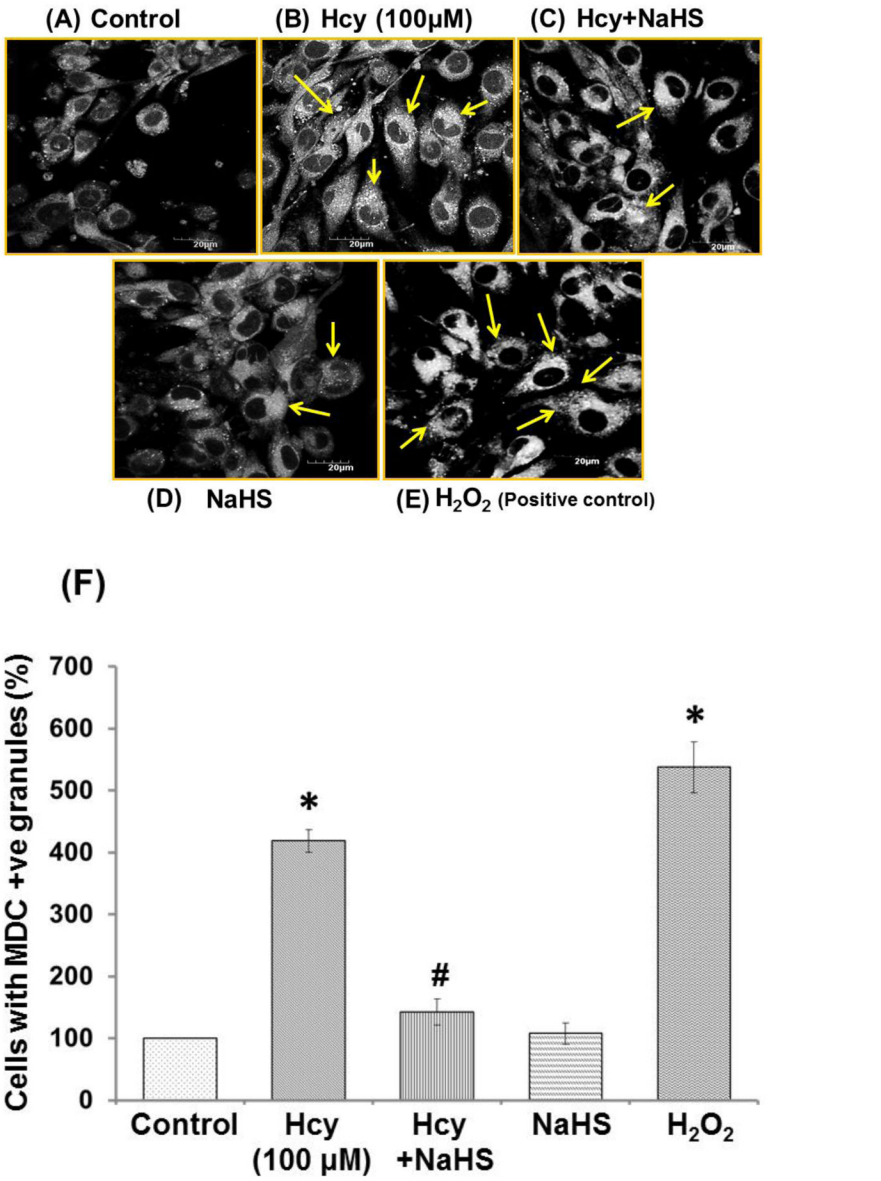

Fig. 12.

Monodansylcadaverine (MDC) staining of autophagosomes under hyperhomocystenemia **(A)** MDC-labeled autophagic structures **(B)** with 100μMHcy, the cells containing MDC-labeled structures increased **(C)** Less autophagic granules is observed in 100μMHcy+NaHS treated group **(D)** NaHS alone treated group **(E)** H_2O_2 treated group showed significant high autophagic granules **(F)** Representative bar diagram statistical analysis of the cells showing autophagic granules and expressed in percentage of control (arbitrary unit). Data represents mean ±SE from n = 4 per group. $^{***}P< 0.0001$ *vs* Control group and $^{\#\#}P< 0.01$ *vs* Hcy treated group.

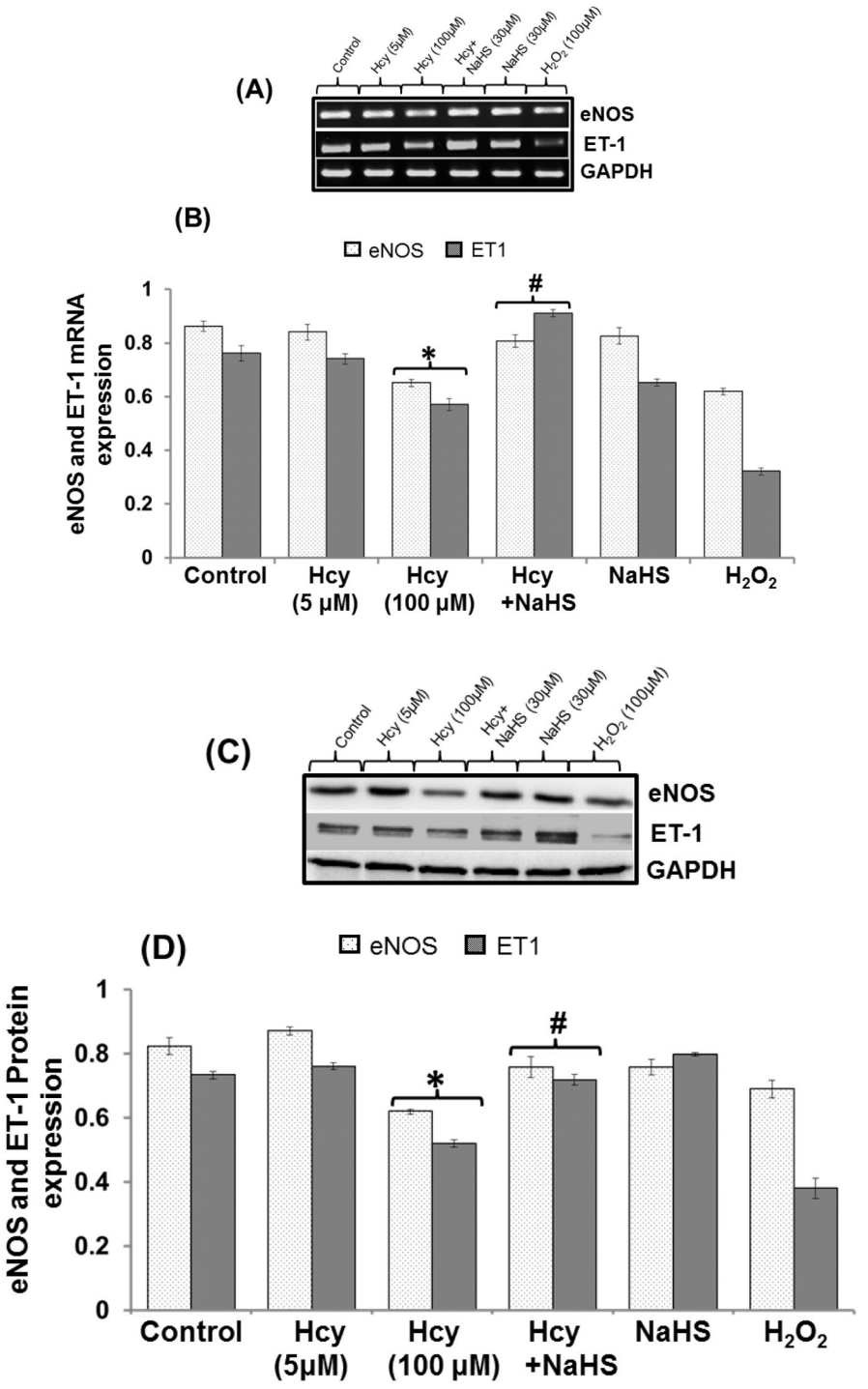

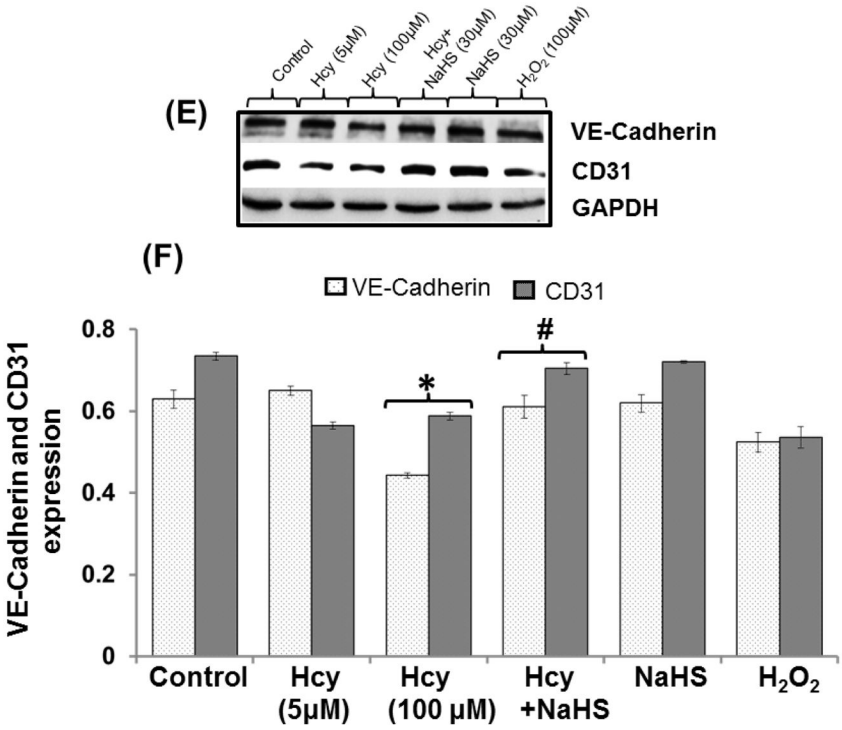

Fig. 13. Exogenous NaHS supplement maintains endothelial function

(A) RT-PCR image denotes eNOS and ET-1 mRNA expression in different treated group of cells **(B)** Densitometry analysis of relative mRNA expression as shown in bar diagram. Figure **(C)** Western blot of eNOS and ET-1 **(D)** Densitometry analysis of eNOS and ET-1 protein expressions **(E)** Western blot analysis showing expression of CD31 and VE Cadherin **(F)** Densitometry analysis of CD31 and VE Cadherin protein. Data represents mean ±SE from n = 4 per group. $^{**}P< 0.005$ *vs* Control group and $^{\#}P< 0.01$, $^{\#\#}P< 0.005$ *vs* Hcy treated group.

Table 1

Primer sequence of different gene

Gene	Primer Sequence (5′-3′)
NR1	Forward: 5′-GAATGATGGGCGAGCTACTCA-3′ Reverse: 5′-ACGCTCATTGTTGATGGTCAGT-3′
eNOS	Forward: 5′-CTGTGGTCTGGTGCTGGTC-3′ Reverse: 5′-TGGGCAACTTGAAGAGTGTG-3′
SOD2	Forward: 5′-GACCTGCCTTACGACTATGG-3′ Reverse: 5′-GACCTTGCTCCTTATTGAAGC-3′
P62	Forward: 5-′GATGTGGAACATGGAGGGAAGAG-3′ Reverse: 5′-AGTCATCGTCTCCTCCTGAGCA-3′
LC3	Forward: 5′-ATGCCGTCCGAGAAGACCTTC-3′ Reverse: 5′-TTACACAGCCATTGCTCGTC-3′
NOX4	Forward: 5′-TGTTGCATGTTTCAGGTGGT-3′ Reverse: 5′-TACTGGCCAGGTCTGCTT T-3
ET1	Forward: 5′-CCCTTTGCAGAATGGATTAT-3′ Reverse: 5′-CTGTAGTCAATGTGCTCGGT-3′
DNA damage M13597/M13361	Forward: 5′-CCCAGCTACTACCATCATTCAAGTAG-3′ Reverse: 5′-GAGAGATTTTATGGGTGTAATGCGGTG-3′
GAPDH	Forward: 5′-ACCACAGTCCATGCCATCAC-3′ Reverse: 5′-TCCACCACCCTGTTGCTGTA-3′